REPORT NO. CG-D-28-78

AN EVALUATION OF SHORE-BASED RADIO DIRECTION FINDING

Charles J. Murphy,
Editor

U.S. DEPARTMENT OF TRANSPORTATION
RESEARCH AND SPECIAL PROGRAMS ADMINISTRATION
Transportation Systems Center
Cambridge MA 02142

SEPTEMBER 1978
FINAL REPORT

Prepared by

U.S. DEPARTMENT OF TRANSPORTATION
UNITED STATES COAST GUARD
Office of Research and Development
Washington DC 20590

NOTICE

This document is disseminated under the sponsorship of the Department of Transportation in the interest of information exchange. The United States Government assumes no liability for its contents or use thereof.

NOTICE

The United States Government does not endorse products or manufacturers. Trade or manufacturers' names appear herein solely because they are considered essential to the object of this report.

Technical Report Documentation Page

1. Report No.	2. Government Accession No.	3. Recipient's Catalog No.
CG-D-28-78		

4. Title and Subtitle	5. Report Date
AN EVALUATION OF SHORE-BASED RADIO DIRECTION FINDING	September 1978
	6. Performing Organization Code
7. Author's Charles J. Murphy, editor	8. Performing Organization Report No. DOT-TSC-USCG-78-8

9. Performing Organization Name and Address	10. Work Unit No. (TRAIS)
U.S. Department of Transportation Research and Special Programs Administration Transportation Systems Center Cambridge MA 02142	CG809/R8003
	11. Contract or Grant No.
12. Sponsoring Agency Name and Address	13. Type of Report and Period Covered
U.S. Department of Transportation United States Coast Guard Office of Research and Development Washington DC 20590	Final Report, January 1977 - April 1978
	14. Sponsoring Agency Code

15. Supplementary Notes

16. Abstract

This report describes an evaluation of Radio Direction Finding (RDF) techniques for shore-based position location performed by the Transportation Systems Center (TSC). The evaluation consisted of the following three phases:

(1) A preliminary survey to identify and classify available direction-finding techniques which could meet Coast Guard requirements;

(2) An analytical modeling and error analysis of the equipment types identified in (1);

(3) Field testing and demonstration of representative equipment.

Major system characteristics considered in the study were:

1. Operational utility of such a system;
2. Cost to implement the system throughout the USCG;
3. Operational impact on the group level - manning and maintenance;
4. Compatibility with existing land lines and VHF-FM remoting capability;
5. Operation in a VHF-FM maritime mobile band;
6. Location of the DF antenna;
7. Ability to home on both voice and EPIRB;
8. Interference effects.

It was concluded that shore-based DF is a valuable potential tool in the accomplishment of SAR mission requirements. Properly implemented shore-based DF can improve reliability and safety of the SAR function by reducing the number of off shore hours necessary to fulfill the mission requirements without increasing station manning requirements.

17. Key Words	18. Distribution Statement
Director Finder, Homer, VHF/FM Marine Band, EPIRB, Search and Rescue	DOCUMENT IS AVAILABLE TO THE U.S. PUBLIC THROUGH THE NATIONAL TECHNICAL INFORMATION SERVICE, SPRINGFIELD, VIRGINIA 22161

19. Security Classif. (of this report)	20. Security Classif. (of this page)	21. No. of Pages	22. Price
Unclassified	Unclassified	90	

Form DOT F 1700.7 (8-72) Reproduction of completed page authorized

PREFACE

This program was performed by personnel of the Communication Branch of the Office of Air and Marine Systems, Transportation Systems Center, for the U. S. Coast Guard. The analysis of direction finding systems was performed by Elie J. Baghdady of Info Systems, Inc., Waltham MA, under agreement with TSC 13651.

The authors wish to recognize the significant contribution of Joseph A. Wolfson of TSC and John R. Carros and Lt. Fred N. Wilder of U.S. Coast Guard Headquarters.

METRIC CONVERSION FACTORS

Approximate Conversions to Metric Measures

Symbol	When You Know	Multiply by	To Find	Symbol
		LENGTH		
in	inches	2.5	centimeters	cm
ft	feet	30	centimeters	cm
yd	yards	0.9	meters	m
mi	miles	1.6	kilometers	km
		AREA		
in^2	square inches	6.5	square centimeters	cm^2
ft^2	square feet	0.09	square meters	m^2
yd^2	square yards	0.8	square meters	m^2
mi^2	square miles	2.6	square kilometers	km^2
	acres	0.4	hectares	ha
		MASS (weight)		
oz	ounces	28	grams	g
lb	pounds	0.45	kilograms	kg
	short tons (2000 lb)	0.9	tonnes	t
		VOLUME		
tsp	teaspoons	5	milliliters	ml
Tbsp	tablespoons	15	milliliters	ml
fl oz	fluid ounces	30	milliliters	ml
c	cups	0.24	liters	l
pt	pints	0.47	liters	l
qt	quarts	0.95	liters	l
gal	gallons	3.8	liters	l
ft^3	cubic feet	0.03	cubic meters	m^3
yd^3	cubic yards	0.76	cubic meters	m^3
		TEMPERATURE (exact)		
°F	Fahrenheit temperature	5/9 (after subtracting 32)	Celsius temperature	°C

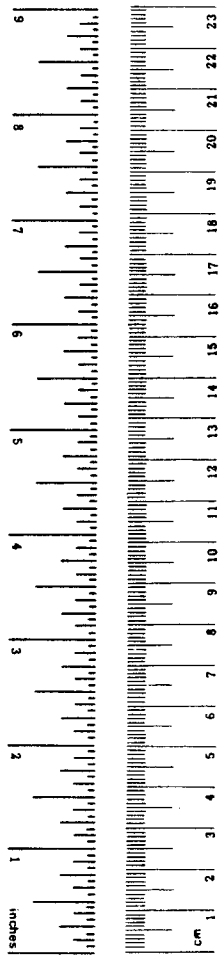

Approximate Conversions from Metric Measures

Symbol	When You Know	Multiply by	To Find	Symbol
		LENGTH		
mm	millimeters	0.04	inches	in
cm	centimeters	0.4	inches	in
m	meters	3.3	feet	ft
m	meters	1.1	yards	yd
km	kilometers	0.6	miles	mi
		AREA		
cm^2	square centimeters	0.16	square inches	in^2
m^2	square meters	1.2	square yards	yd^2
km^2	square kilometers	0.4	square miles	mi^2
ha	hectares (10,000 m^2)	2.5	acres	
		MASS (weight)		
g	grams	0.035	ounces	oz
kg	kilograms	2.2	pounds	lb
t	tonnes (1000 kg)	1.1	short tons	
		VOLUME		
ml	milliliters	0.03	fluid ounces	fl oz
l	liters	2.1	pints	pt
l	liters	1.06	quarts	qt
l	liters	0.26	gallons	gal
m^3	cubic meters	35	cubic feet	ft^3
m^3	cubic meters	1.3	cubic yards	yd^3
		TEMPERATURE (exact)		
°C	Celsius temperature	9/5 (then add 32)	Fahrenheit temperature	°F

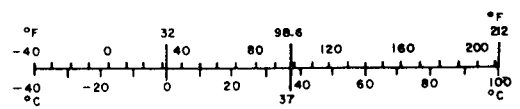

TABLE OF CONTENTS

Section		Page
1.	INTRODUCTION	1-1
2.	DIRECTION FINDING SYSTEM MODELS	2-1
	2.1 EPIRB DF System Requirements	2-1
	2.2 Types and Makes of RDF Equipment Considered in Present Analysis	2-2
	2.3 Fundamentals of Doppler RDF Technique	2-2
	2.3.1 Basic Theory of Doppler RDF	2-2
	2.3.2 Required Number of Antennas	2-7
	2.3.3 Methods of Doppler RDF Reception	2-9
	2.3.4 Summary of Design Characteristics of Commercial Doppler RDF Equipment	2-9
	2.4 Fundamentals of Adcock RDF Techniques	2-14
	2.5 Fundamentals of Homer-Type RDF Techniques	2-15
	2.6 Models of Propagation and Multisignal Receiving Environments	2-19
	2.6.1 Multipath Propagation	2-19
	2.6.2 Electromagnetic Environment	2-21
3.	ERROR ANALYSIS	3-1
	3.1 Sources of Error in RDF Systems	3-1
	3.1.1 Common Error Sources	3-1
	3.1.2 Error Sources Peculiar to Doppler RDF Technique	3-1
	3.1.3 Error Sources Peculiar to Adcock and Homer RDF Techniques	3-2
	3.2 Analysis of Doppler RDF Systems	3-2
	3.2.1 Random Noise Effects	3-2
	3.2.2 Error Due to Overlap of Voice Spectrum With f_m	3-4
	3.2.3 Site Effects: Direct Plus Specular-Reflected Paths	3-5
	3.2.4 Site Effects: Direct Plus Two or More Specular-Reflected Paths	3-11
	3.2.5 General Observations Regarding Errors Caused by Off-Azimuth Reflectors	3-13
	3.2.6 Co-channel and Off-channel Interference	3-14
	3.2.7 Effects of Sea State	3-15

TABLE OF CONTENTS (CONTINUED)

Section		Page
	3.3 Analysis of Adcock RDF System	3-16
	3.4 Analysis of Homer System	3-19
4.	EXPERIMENTAL PROGRAM	4-1
	4.1 Introduction	4-1
	4.2 Field Tests	4-3
	4.2.1 Shore-Based RDF Tests at Winthrop Highlands, Massachusetts	4-3
	4.2.2 Tests Conducted with Homer Equipped Cutter	4-12
	4.2.3 Tests Conducted with Homer Equipped Helicopter	4-14
	4.3 System Demonstration at USCG Station, Pt. Allerton, Massachusetts	4-17
	4.3.1 Site Preparation	4-17
	4.3.2 System Demonstration	4-17
5.	CONCLUSIONS AND RECOMMENDATIONS	5-1
	APPENDIX A - EQUIPMENT SPECIFICATIONS	A-1
	APPENDIX B - IDFM POSITION DETERMINATION SYSTEM	B-1
	REFERENCES	R-1

LIST OF ILLUSTRATIONS

Figure		Page
2.3.1	Illustration of Dependence of Phase of Doppler Induced Sinewave Upon the Azimuth of Incidence of the Signal	2-3
2.3.2	Basic Functional Structure of a Doppler RDF System	2-4
2.3.3	Simulation of Receiving Antenna Rotation by Commutation of Receiver Input Among N Discrete Circularly Arranged Antennas	2-6

LIST OF ILLUSTRATIONS (CONTINUED)

Figure		Page
2.3.4	Illustration of the Spectrum at the Output of the Antenna Commutator.....	2-6
2.3.5	Major-Function Structure of Rohde and Schwarz System.....	2-11
2.4.1	Pictorial Diagram of the OAR Adcock Direction Finder (Center Antenna is the "Sense" Antenna)...	2-16
2.5.1	Intersecting Directional Antenna Patterns for Homing-Type RDF.....	2-17
2.5.2	Major-Function Structure of the Dorne and Margolin Homer System.....	2-18
3.2.1	Geometry of Direct Plus One Specular-Reflected Paths.....	3-6
3.3.1	Geometry of a Pair of Antennas in an Adcock RDF System, with Incident Direct and Reflected Rays.....	3-17
4.1	Test Site at Winthrop, Massachuestts.....	4-4
4.2	Servo Corp. DF Antenna Mounted on Test Van.....	4-4
4.3	Diagram of Shore-Based Direction Finder Tests.....	4-5
4.4	Diagram of Signal Strength Measurement System....	4-6
4.5	DF Bearing Error vs Range in Nautical Miles - Typical Performance.....	4-8
4.6	DF Bearing variation vs Range in Nautical Miles, Typical Performance - Received Signal Level in dBM Noted Under Variation Bars.....	4-9
4.7	Antenna Height vs Range for Transmitting Antenna on Surface.....	4-10
4.8	DM SE47-7 VHF/FM Homing System.....	4-13

LIST OF ILLUSTRATIONS (CONTINUED)

Figure		Page
4.9	Forty-One Foot Cutter With Homer Installed.....	4-15
4.10	HH-52 Helicopter Used In Homing Tests.....	4-15
4.11	Homer Antenna Installation on HH-52 Helicopter..	4-16
4.12	DF Antennas Deployed on Roof of Point Allerton Station: (1) Servo; (2) Intech; (3) OAR.....	4-19
4.13	Installation of Servo Corp. antenna with Intech Antenna Mounted Above.....	4-20

LIST OF TABLES

Table		Page
2.1	DESIGN COMPARISON OF DOPPLER DF EQUIPMENT.....	2-10
4.1	COMMERCIALLY AVAILABLE VHF-FM DIRECTION FINDERS.....	4-2
4.2	MAXIMUM RANGES ACHIEVED IN DF & HOMING TESTS.....	4-18

1. INTRODUCTION

The U.S. Coast Guard in seeking improvements in search and rescue (SAR) capability seeks to reduce the emergency notification (alerting) time for an individual distress and provide improved capability for detecting and locating the distress. Presently the Coast Guard is actively pursuing the regulatory actions necessary to allow carriage of an Emergency Position Indicating Radio Beacon (EPIRB) compatible with the maritime VHF-FM system by certain ships and boats operating within the radio coverage of the National VHF-FM Distress System. In support of the VHF-FM EPIRB system the feasibility of a cost effective locating and direction finding capability to be incorporated within the VHF-FM Distress System is being examined.

This report describes an evaluation of Radio Direction Finding (RDF) techniques for shore-based position location performed by the Transportation Systems Center (TSC). The evaluation consisted of the following three phases:

(1) A preliminary survey to identify and classify available direction-finding techniques which could meet Coast Guard requirements;

(2) An analytical modeling and error analysis of the equipment types identified in (1);

(3) Field testing and demonstration of representative equipment.

Major system characteristics to be considered in the study are:

1. Operational utility of such a system.
2. Cost to implement the system throughout the USCG.
3. Operational impact on the group level - manning and maintenance.
4. Compatibility with existing land lines and VHF-FM remoting capability.
5. Operation in a VHF-FM maritime mobile band.
6. Location of the DF antenna.
7. Ability to home on both voice and EPIRB.
8. Interference effects.

Upon initial investigation it was determined that existing DF equipment could be broadly classified into three catagories:

(1) RDFs employing the pseudo doppler principle;

(2) RDFs employing the Adcock principle;

(3) Homing devices furnishing a left-right indication instead of a bearing.

Complete specifications were obtained on the available equipment in the above categories wherever possible and are included as Appendix A.

In Section 2, entitled Direction Finding System Models, the system-level requirements for a DF system in the EPIRB application are outlined based on a preliminary concept of EPRIB signaling and reception modes under consideration by TSC. The DF systems included in the present analysis are then identified and their functional models and critical design and performance parameters are determined. Finally, the propagation and signal reception environment is modeled, including the interference threat presented by probable spectral congestion and unfavorable signal levels (due to a variety of operational causes) for the distress signal relative to signals from other active sources.

In Section 3, entitled Error Analysis, error expressions are derived for each type of system or DF technique considered, and the results are applied to the specific equipment embodiments singled out for evaluation. The error causes considered are two types: Those peculiar to the DF technique and those common to all techniques (such as multipath, multi-signal interference and certain propagation anomalies).

Section 4 describes field tests conducted with commercially available equipments representative of the three categories analyzed in Sections 2 and 3. The purpose of these tests was to demonstrate the capabilities of a shore-based direction-finding system. Due to limitations in resources, the tests and the resulting data were of a very basic nature and as such did not consitute a detailed performance evaluation or a comparative evaluation of the equipment selected for the tests. (The program originally did not include the field tests, which were added later when it became apparent that sufficient funds for limited testing would be available).

Section 5 summarizes the analytical and experimental results and presents conclusions and recommendations both for further experimentation and operational installations of shore-based DF systems.

Appendix B describes a position determination system developed by Elie Baghdady in 1970 which enables high accuracy determination of direction and distance to the source by means of frequency measurements with baseline dimensions of about ten meters.

2. DIRECTION FINDING SYSTEM MODELS

2.1 EPIRB DF System Requirements

A distress signal emanting from an offshore emergency radio beacon source could provide an invaluable aid to the determination of the direction in which rescue craft must head in order to find the source. Typically this would require a shore-based direction finder together with suitable equipment aboard small surface craft and helicopters.

TSC is engaged in the development of a system design specification for an Emergency Position Indicating Radio Beacon (EPIRB) system based on utilizing channels 15 (156.750 MHz) and 16 (156.800 MHz) of the VHF Marine FM Mobile Band. A tentative EPIRB signal format being considered by TSC consists of transmitting an "alert" signal for two seconds on channel 16 (the designated national distress channel) and following up with a 15-second "locate" signal on channel 15. The coverage range requirement is shore to radio horizon (up to 20 nautical miles) for all U.S. Coastal areas, including the Great Lakes.

The leading candidate source location aid is radio direction finding (RDF) equipment, preferably commercially available "off-the-shelf" hardware. A minimal amount of state-of-the-art development or equipment modification or retrofit is not ruled out if sufficiently desirable.

The RDF system must provide high resolution and accuracy in a receiving site environment that is generally encumbered with reflectors (trees, power lines, buildings, towers, etc.) that cause a serious multipath threat, and in an electromagnetic environment that may cause multi-signal conditions as a result of simultaneous occupancy of the EPIRB channels and/or relative distances to different transmitters in combination with limited receiver dynamic range.

For the purposes of this program, the following requirements were provided by the Coast Guard:

a. Signal Sensitivity - equivalent to VHF receivers presently in use at Coast Guard shore stations;

b. Accuracy - ± 3 degrees rms;

c. Mechanical/structural - suitable for installation on unattended antenna towers, over the range of environmental conditions prevalent in the U.S.

2.2 Types and Makes of RDF Equipment Considered in Present Analysis

A number of radio direction finding techniques have long been in use in existing equipment. Among these, the following have been singled out for error analysis and comparison:

a) Doppler Technique, examplified by
- Rohde & Schwarz VHF Direction Finder NP7
- Servo Corporation of American Model 7030 VHF/UHF Direction Finder System
- Pilot Instrument Corporation Model 804RA-7 Marine VHF Direction Finder

b) Adcock Technique, examplified by
- O. A. R. Model ADFS-320 Automatic Direction Finder

c) Homing Technique, examplified by
- Dorne & Margolin, Inc. DM SE47-7 VHF/FM Homing System

2.3 Fundamentals of Doppler RDF Technique

2.3.1 Basic Theory of Doppler RDF

The Doppler RDF equipment considered in this study are all based on the principle that if the receiving antenna executes a circular motion at a uniform angular velocity, this motion will induce in the received signal a sinewave frequency modulation at the angular frequency of the antenna rotation, the phase of the sinewave modulation waveform being determined by the azimuthal angle of incidence of the received signal. Reference to Figure 2.3.1 shows that the zeros of the sinewave Doppler-shift frequency modulation induced in the signal S_1 arriving from the S_1-O direction correspond to the instants of time at which the rotating receiving antenna crosses positions A and A', whereas for signal S_2 arriving along the direction

of S_2-O, the zero crossings of the modulation waveform occur in time at the instants when the rotating receiving antenna crosses points B and B'. Accordingly, if the direction of O-N is taken as reference, the phase of the S_1 sinewave relative to the phase of a sinewave of the same frequency which corresponds to the induced FM of a signal arriving along N-O is equal to θ_1.

The basic functional structure of a Doppler RDF system is illustrated in Figure 2.3.2. With reference to this figure, the azimuth angle of arrival of an incident wavefront at frequency f_c is automatically converted into the "initial phase", θ, of a sinewave by rotating the receiving antenna A at the rate of f_m cycles per second around a circle of radius r. The rotation induces a sinusoidally varying Doppler shift given by

$$f_{d,\max} \sin (2\pi f_m t - \theta) \tag{2.1}$$

where

$$f_{d,\max} = 2\pi f_m (r/\lambda_c) \ , \ \lambda_c = c/f_c \tag{2.2}$$

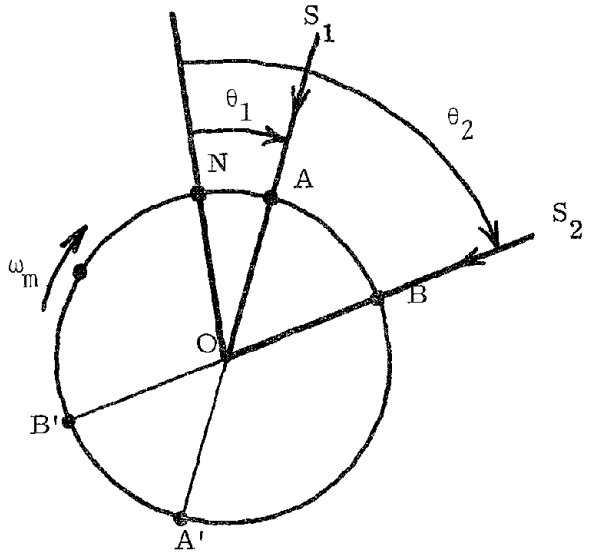

FIGURE 2.3.1 ILLUSTRATION OF DEPENDENCE OF PHASE OF DOPPLER INDUCED SINEWAVE UPON THE AZIMUTH OF INCIDENCE OF THE SIGNAL

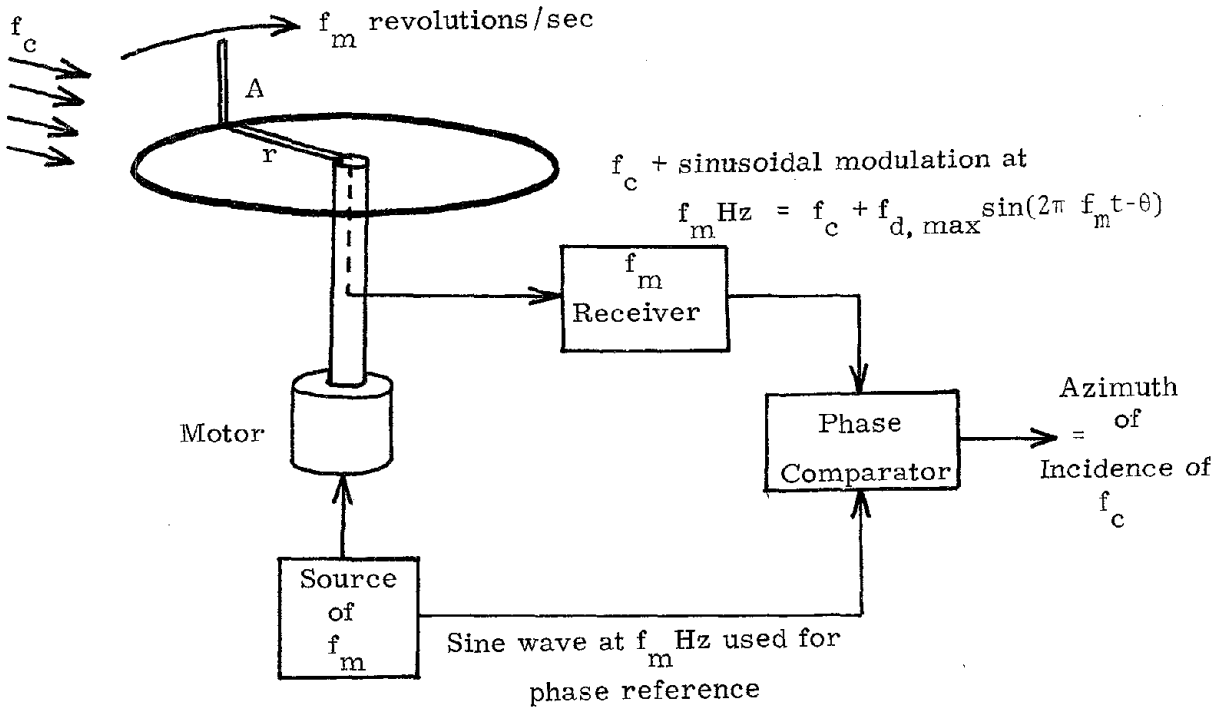

FIGURE 2.3.2 BASIC FUNCTIONAL STRUCTURE OF A DOPPLER RDF SYSTEM

and the "initial phase" (i. e., phase for t=0), , of the sinusoidal Doppler modulation equals the azimuth of incidence of the received wavefront relative to the reference direction set by the phase of the reference f_m - Hz sinewave.

As illustrated in Figure 2.3.3, the antenna rotation is actually simulated by electronically commutating the receiver input among N discrete antennas arranged around the circumference of the circle. This commutation in effect samples the incident signal f_m times per second at each of N delay phase-shifted replicas of this signal that are sensed at the N circularly arranged antenna positions. The result is equivalent to $f_s = Nf_m$ samples/sec of the incident signal with a time-variant delay phase shift given by

$$(f_{d,\,max}/f_m) \cos (2\pi f_m t - \theta) \qquad (2.3)$$

added to its RF phase.

Alternatively, the commutation process can be viewed as the process of providing $f_s = Nf_m$ discrete samples/sec of the desired continuous rotation of the receiving point around the circumference of the circle.

Indeed, it can readily be shown that the signal delivered by the commutator to the receiver is equivalent to the signal delivered by a continuously rotating receiving antenna, sampled at the rate of $f_s = Nf_m$ samples per second, and hence has a spectrum of the form illustrated in Figure 2.3.4.

It is important to note, however, that the instantaneous frequency difference between any two adjacent zones is always f_s, because the frequency modulation waveforms (i. e. the voice waveform and the induced sinusoidal Doppler shift waveform) of any one of the spectral zones are

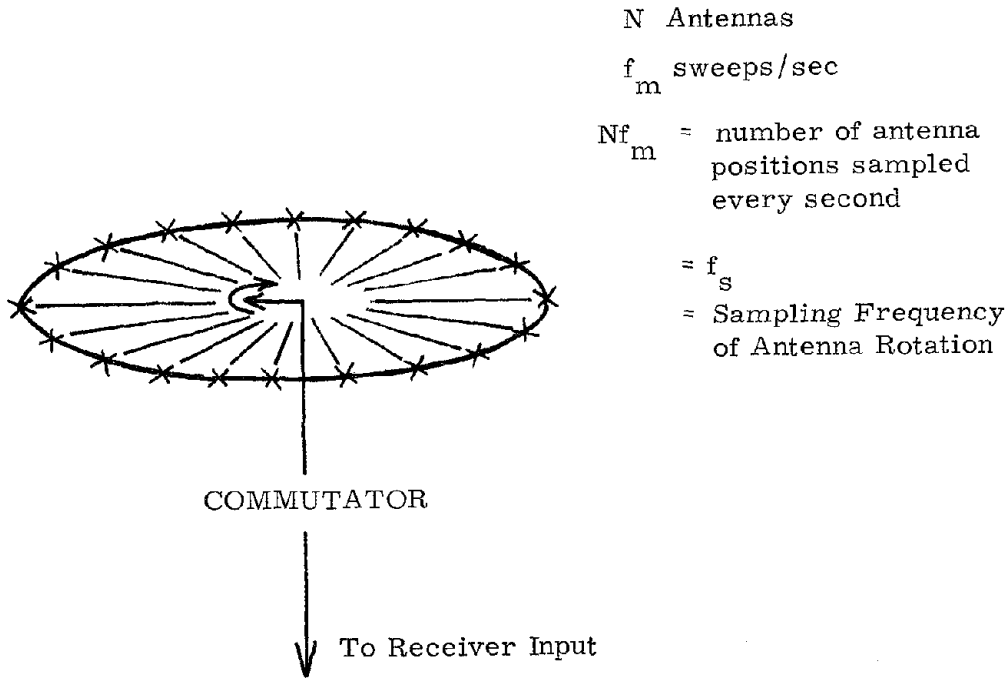

FIGURE 2.3.3 SIMULATION OF RECEIVING ANTENNA ROTATION BY COMMUTATION OF RECEIVER INPUT AMONG N DISCRETE CIRCULARLY ARRANGED ANTENNAS

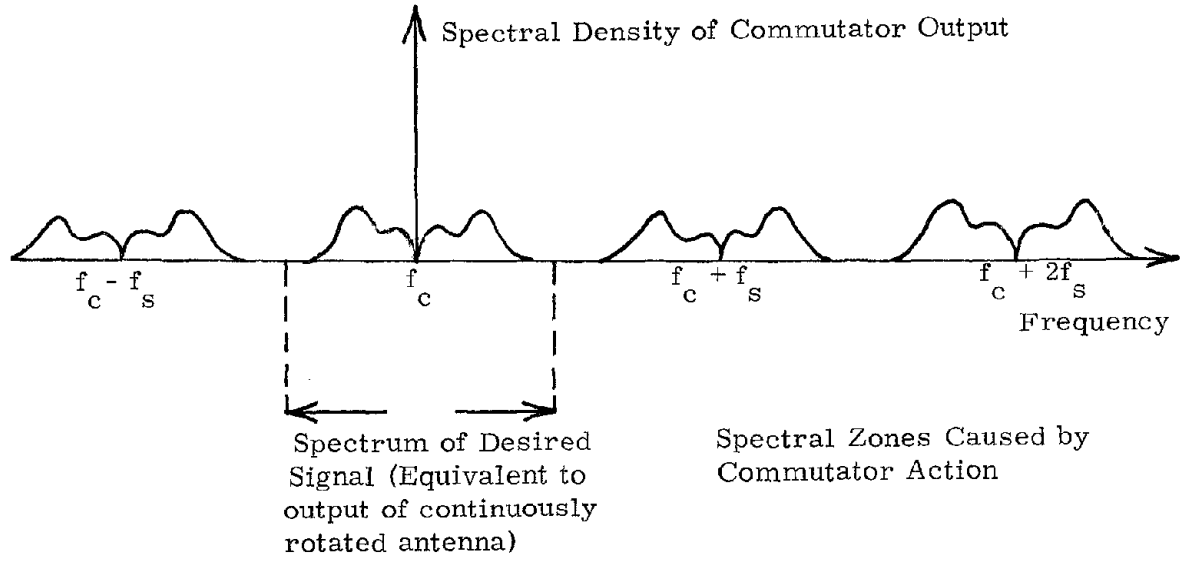

FIGURE 2.3.4 ILLUSTRATION OF THE SPECTRUM AT THE OUTPUT OF THE ANTENNA COMMUTATOR

instantaneously identical (in magnitude and phase) from one spectral zone to the next, and hence cancel out in the instantaneous frequency difference, leaving only the sampling frequency, $f_s = Nf_m$) as the value of the instantaneous frequency between any two adjacent spectral zone signals. This means that if the receiver design characteristics satisfy the requirements for high capture (almost a capture ratio of 1), then the effects of the inter-zone interference on the output of the FM demodulator will all be filterable (i.e., rejectable) if $f_s = Nf_m$ exceeds the output post-detection filter bandwidth. For the DF f_m - Hz tone extraction, the latter condition means $f_s = Nf_m > f_m$, which holds for all $N > 1$. However, for the voice waveform, $f_s = Nf_m$ must exceed the highest voice frequency of interest, which is usually somewhere between 3,300 and 4000 Hz.

The above observations not only help us understand the nature and characteristics of the signal delivered by the commutator to the receiver input, but also provide the rigorous analytical basis for determining the minimum number N of antennas that must be provided, the maximum allowable spacing between antennas, the consequences of not observing these conditions on N and the antenna spacing, the conditions to be observed in the design of the receiver filters, and the mechanism of potential mutual interference among incident signals even when they are widely different in frequency.

2.3.2. Required Number of Antennas

With reference to Figure 2.3.4, it is clear that in order to ensure that the sampling spectral zones are "disjoint" or separable one from the others by means of fixed time-invariant receiver pre-detection filters, the number N of commutated discrete antennas must satisfy the condition

$$Nf_m > \text{(Bandwidth, } B_s\text{, of Signal Out of Continuously Rotating Antenna)} \qquad (2.4)$$

The antenna rotation rate, f_m, is chosen either above the voice band or less than the lowest voice frequency passed

In general, the incident signal is frequency modulated by voice for operation in the frequency band of interest. However, if deemed desirable, as will be indicated by the results of this study, the frequency modulation may be either wiped off in the receiving system, or inhibited at the transmitting end for aiding the direction finding function. Accordingly, we distinguish two situations, as follows, for determining the minimum value of N according to condition (2.4).

Condition A

If the incident wave is an unmodulated carrier, or if the voice modulation is wiped off prior to FM demodulation, then

$$B_s \approx 2\left[f_{d,\,max} + f_m\right] \text{ if } \delta = f_{d,\,max}/f_m \text{ is } >> 1 \text{ or } << 1$$
$$\approx 2f_m(1+\delta) = 2f_m\left[1 + 2\pi(r/\lambda_c)\right] \qquad (2.5)$$

Therefore we must have

$$N > 2(1+\delta) = 2\left[1 + 2\pi(r/\lambda_c)\right] \qquad (2.6)$$

for $\delta \equiv 2\pi(r/\lambda_c) >> 1$ or $<< 1$

Condition B

If the incident wave is modulated, and this modulation is not wiped off prior to FM demodulation, then we must have

$$N > B_s/f_m \qquad (2.7)$$

2.3.3 Methods of Doppler RDF Reception

Two reception techniques are indicated for Doppler RDF:

1. Pre-demodulation voice modulation wipe-off, followed by FM demodulation to extract the induced Doppler modulation waveform (the sinewave at f_m Hz); and

2. Combined FM demodulation of both voice and induced sinusoidal FM, followed by filter separation of the voice and induced Doppler modulation waveform

Technique 1 is preferred because

a) It allows the number of antennas to be reduced to the value required by Condition (2.6) on N.

b) It allows pre-demodulation bandwidth to be reduced to $2f_m(1+\delta)$ when f_m is below the lowest voice frequency, which reduces the noise threshold and the receiver vulnerability to interference.

2.3.4 Summary of Design Characteristics of Commercial Doppler RDF Equipment

The design characteristics of three leading makes of Doppler RDF are summarized in Table 2.1. The equipment listed in this table are the models identified in Section 2.2. Potentially significant design characteristics of each of the three direction finders listed in Table 2.1 will now be brought out and their significance discussed.

Rohde & Schwarz

The major-function structure of the Rohde & Schwarz D. F. NP7 is brought out in Figure 2.3.5.

In addition to the circular sequence of antennas that is characteristic of a Doppler RDF, the D. F. NP7 utilizes an additional antenna at the center of the circle to receive the incident signal in the conventional

TABLE 2.1 DESIGN COMPARISON OF DOPPLER DF EQUIPMENT (For f_c = 156.750 MHz, λ_c = 1.914 m)

EQUIPMENT	r (m)	f_m (Hz)	δ	$f_{d,max}$ (Hz)	$B_{S,D} = 2f_m(1+\delta)$ (Hz)	N	f_s (Hz)	($f_s > B_{S,D}$) Condition (2.6) N >	($f_s > B_S$ = 15KHz) Condition (2.7) N >
ROHDE & SCHWARZ	3	170	9.85	1674.5	3689	32	5440	21	88
SERVO CORP OF AMERICA	1.568	216	5.15	1112.4	2657	16	3456	12	69
PILOT	0.038	3500	0.125	436.6	7875	4	14000	2	4

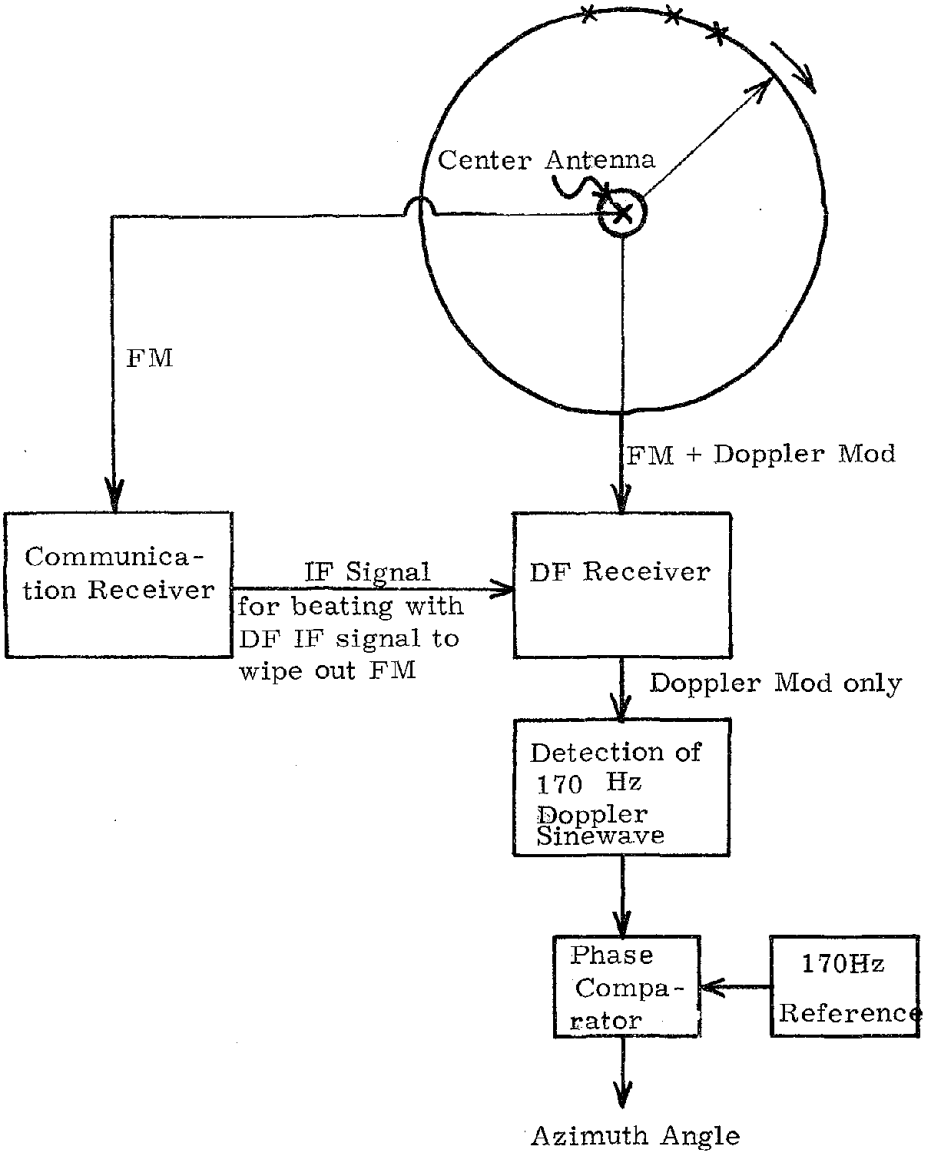

FIGURE 2.3.5 MAJOR-FUNCTION STRUCTURE OF ROHDE AND SCHWARZ SYSTEM

manner for use to cancel out the voice modulation of the signal applied by the commutator to the receiver input before reaching the FM demodulator. This ideally would result in the carrier in each of the spectral zones being modulated only by the induced sinusoidal FM by sinewave at f_m Hz before applying it to the final FM demodulator. Accordingly, all of the energy of each sampling spectral replica of the incident FM signal becomes concentrated in a signal within the significantly narrower bandwidth of an FM by sinewave at f_m Hz where f_m is less than 1/10 of the voice bandwidth. The following benefits result:

a) The desired commutation spectral zone becomes more effectively separable from the other spectral zones on both sides of it, which eliminates inter-zone interference.

b) The narrower pre-demodulator signal bandwidth means lower pre-demodulator effective noise and cochannel/offchannel interference bandwidth. Consequently, the noise threshold for obtaining f_m is significantly reduced, and the probability of interference from off-channel signals is also effectively reduced. The threshold reduction of course means proportionately increased range.

Servo Corporation

In the Servo Corporation Model 7030, no pre-demodulation "wipe-off" of the voice modulation is attempted. Rather, the signal with the combined FM modulation by voice and the Doppler induced direction-finding sinusoidal f_m - Hz modulation is demodulated by a "high-performance linear FM discriminator detector." Since (see Table 2.1) the commutator sampling frequency in this case is $f_s = 16 \times 216 = 3,456$ Hz, and since FM with an rms frequency deviation of 3.5 kHz (or a "peak" frequency deviation of 5 kHz) by a nominal 4-kHz voice band results in a value of $B_{S, V+D}$ much greater than f_s, it is clear that the $f_c \pm f_s$ commutation spectral

zones will severly overlap the f_c zone, and hence will not be totally suppressible before demodulation. Moreover, the noise and cochannel interference bandwidth will be the total IF bandwidth required to accommodate the signal with FM by both voice and the direction-finding sinusoidal induced Doppler.

The Servo system must therefore rely entirely on the capture characteristics of the "high-performance linear FM discriminator detector" to suppress the unavoidable inter-zone interference and isolate the desired f_m-Hz direction-finding sinewave without any phase error on it.

Pilot Direction Finder

In the Pilot system, the value of f_m is chosen on the higher side of the voice spectrum, which results in a value of f_s = 14000 Hz. This high value of f_s eases the problem of predemodulation separation of the desired spectral zone, and reduces the minimum required number of antennas to the few (4) actually used. Moreover, in view of the high value of f_m, there is no real advantage in modulation wipe-off prior to demodulation. Thus, the noise threshold of the Pilot system should more likely exceed than equal that of the Servo system. The very small value of DF signal modulation index(because of the very small radius of the circle) should also make the Pilot system much more vulnerable to site effects and to interference from cochannel and offchannel signals than the other two systems.

2.4 Fundamentals of Adcock RDF Techniques

The Adcock antenna consists of spaced vertical open antennas, which in principle respond only to one (the vertical) component of polarization of an incident wavefront and hence is not subject to the polarization errors that plague loop antennas. Indeed, except for a reduction in effective antenna height, a two-element Adcock antenna is equivalent to a frame antenna with its top horizontal arm removed. Thus, a two-element Adcock should be free of the pattern distortion and null displacement and/or blurring effects encountered with loop antennas in the reception of "abnormally" polarized, obliquely incident wavefronts.

The two-element Adcock consists of two vertical elements, spaced not more than $\lambda/2$, mounted on rotatable assembly, or driving a goniometer. Two such Adcocks mounted so that their planes are mutually orthogonal form a crossed Adcock configuration.

In crossed Adcocks in which the resultant of each pair of vertical elements drives a field coil of a goniometer, the spacing between the elements of a pair must be limited in order to approximate the $\cos\theta$ and $\sin\theta$ functions required to make the angle indicated by the shaft of the search coil approximate the azimuth angle of arrival of the incident wavefront. Since for arbitrary spacing, the voltage delivered by the reference pair will vary with θ as $\sin\left[(\phi_o/2)\cos\theta\right]$ while that delivered by the orthogonally situated pair will vary as $\sin\left[(\phi_o/2)\sin\theta\right]$, the angle α indicated by the shaft position of the search coil will be given by

$$\tan\alpha = \frac{\sin\left[(\phi_o/2)\sin\theta\right]}{\sin\left[(\phi_o/2)\cos\theta\right]}$$

$$\simeq \tan\theta, \qquad \text{for } \phi_o \equiv 2\pi L/\lambda \leq \pi/2 \text{ rad}.$$

The difference between α and θ is an error in bearing indication. The restriction on ϕ_o to keep this error small signifies a separation $L \leq \lambda/4$ between elements of a pair.

Adcock antennas have physical appearances of U or H for combined pairs, and may combine several such pairs.

A pictorial diagram of the OAR VHF Band Automatic Direction Finder Model ADFS-320 is shown in Figure 2.4.1. The standard Adcock antenna array is for shipboard or shore-station installation. It consists of 4 vertical dipole elements and a central whip for sense reference (i. e., for resolving the 180-degree directional ambiguity). This sense ambiguity resolution is performed automatically by special circuits without manual intervention.

2.5 Fundamentals of Homer-Type RDF Techniques

In the homing technique, two directional receiving antennas are employed as illustrated in Figure 2.5.1, with polar patterns directed along different directions making an acute angle, the two patterns intersecting along the boresight axis or the centerline of the mount or vehicle to be oriented toward the beacon source. The receiver input alternates between the two antennas at a rapid rate. If the direction of arrival of the incident signal is not coincident with the axis of intersection 0-0' in Figure 2.5.1, then, as illustrated by the line O-S, the amplitudes of the signal as delivered by each antenna will be different. Accordingly, the received signal amplitude will be stepped between different levels by the antenna switching. Only when O-O' is steered to coincide with O-S will the signal amplitudes from the two antennas be identical, and hence no amplitude changes or jumps will be imparted to the received signal by the antenna switching operation.

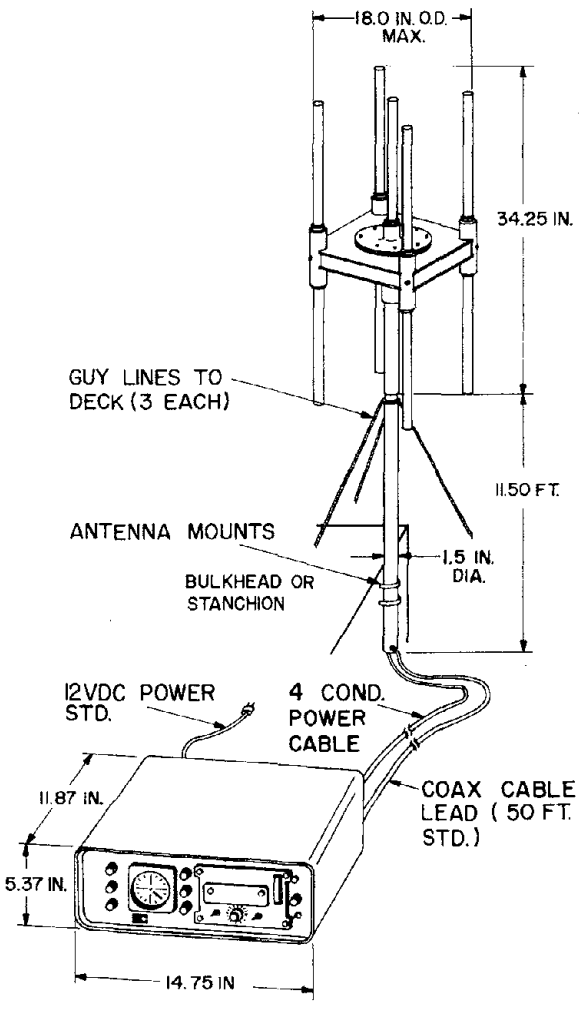

FIGURE 2.4.1 PICTORIAL DIAGRAM OF THE OAR ADCOCK DIRECTION FINDER (CENTER ANTENNA IS THE "SENSE" ANTENNA)

Source: Ocean Applied Research Corporation, Product Bulletin 1-75

The detected jumps in amplitude are applied to a "homing indicator" that is adjusted to show a centerline (or "on course") indication if O-O' is lined up with O-S, and a left or right indication depending on which of the two lobes is pointed more toward the direction of incidence of the homing beacon wavefront.

A simplified functional diagram of the Dorne and Margolin DM SE47-7 VHF/FM Homing System is shown in Figure 2.5.2. In this system, the antenna switching and the corresponding Homing Indicator gating are controlled by a 1.8 KHz square wave generated by a free-running multivibrator.

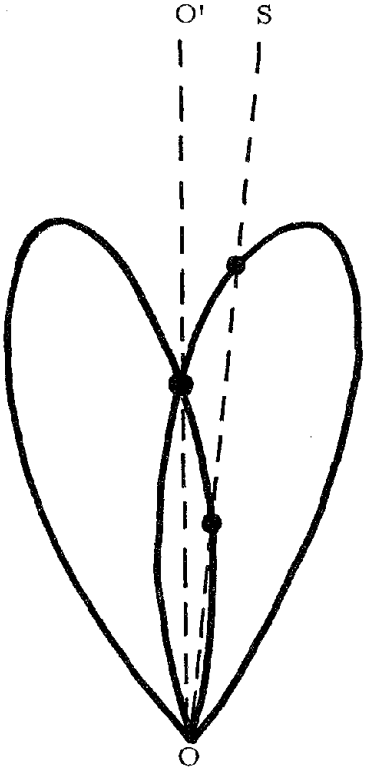

FIGURE 2.5.1 INTERSECTING DIRECTIONAL ANTENNA PATTERNS FOR HOMING-TYPE RDF

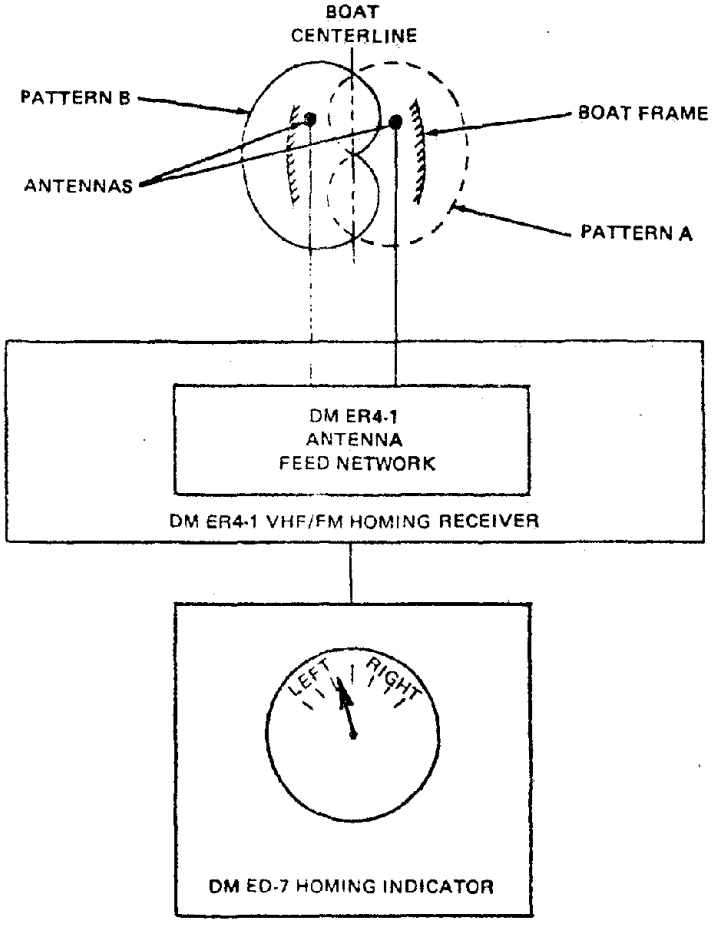

FIGURE 2.5.2 MAJOR-FUNCTION STRUCTURE OF THE DORNE AND MARGOLIN HOMER SYSTEM

2.6 Models of Propagation and Multisignal Receiving Environments

2.6.1 Multipath Propagation

In the analysis of RDF systems, we distinquish two types of multipath: Multipath caused by reflections off the intervening (generally, water) surface, and multipath caused by reflections by site features (such as trees, buildings, towers, power lines, etc.).

Paths caused by ordinary intervening surface reflections generally fall in the same azimuthal (vertical) plane as the main line-of-sight (LOS) incident ray path. Therefore, such paths do not cause a "pulling effect" on the azimuth indication of the main LOS path, and hence do not cause an azimuth "pulling" error. However, multipath of this type will generally cause relatively slow envelope fading which, because of the very small reflected-path grazing angles involved, is much shallower for vertically polarized signals than for horizontally polarized signals.

Only reflectors that yield signals that arrive from "off-path" directions that are significantly different from the direction of the direct line-of-sight path present a threat of significant DF performance degradation. Such reflectors usually are present at or in the vicinity of the DF receiver site and include such natural and man-made features as hillsides, cliffs, high rock or earth piles or dunes, buildings, towers, power lines, fences, etc. Reflections from structures on a boat transmitting the distress signal definitely affect the resultant transmitting antenna pattern by causing lobing characteristics, but the lateral dimensions of boats and their structures are generally so small compared to distances to the DF receiving site that the differences between their azimuthal angles of arrival and that of the direct LOS path are too small to cause any noticeable azimuth pulling errors.

The term "site effects" is commonly employed in reference to reflections from surrounding terrain features at the DF receiving site. The use of elevated antennas to clear obstacles and tower over, and hence reduce, the effect of surrounding reflecting terrain features enhances the reception of "ground" reflected rays. Lobe formation with nulls in low-angle-coverage caused by interference between direct and intervening-ground-reflected rays is usually minimized by mounting the antenna system a few feet above a counterpoise. However, the area illuminated by the first Fresnel zone usually extends beyond the counterpoise, and significant ground reflections may still be received. Thus, if the counterpoise is not elevated too high (i.e., not higher than around 15 feet), only the lowest part of the first lobe is formed an no serious nulls result. However, more and finer lobes with nulls in low-angle coverage could be formed if the counterpoise is placed at higher elevations. Thus, although the use of elevated antennas may appear to be an effective way to reduce site effects, this measure will fail if low coverage-angle nulls develop as a result of excessive elevation, which would create narrow zones of relatively weak direct-path signals where the performance therefore becomes much more susceptible to off-path reflections.

The surrounding terrain and water surface will give rise to specular reflections provided the surface roughness, measured by a ripple depth Δh, say, satisfies the (Rayleigh) criterion

$$\Delta h < \frac{\lambda}{16 \sin \psi}$$

where λ is the incident wavelength, and ψ is the grazing angle. For a grazing angle of 0.1 rad, this criterion requires $\Delta h < 1.2$ meters for Channel 15 and 16 frequencies.

The Rayleigh criterion can also be applied to off-path site reflectors. Thus if the roughness of the reflecting surface is measured by Δh, then since the grazing angle for off-path side reflectors can be as high as 45 degrees, the criterion for specular reflection becomes (for Channel 15 and 16 frequencies)

$$\Delta h < \lambda / 22.63 \approx 8.5 \text{ cm} \quad \text{for } \psi = 45^{\circ}.$$

2.6.2 Electromagnetic Environment

Channels 15 and 16 will generally be available to anyone in distress. In time of a regional storm, there could be a multiplicity of craft (boats, ships) in need of emergency assistance scattered so that they are all within LOS range of a shore DF station. A real interference threat is therefore likely among simultaneous users of the EPIRB channels.

One complicating factor of the mutual interference threat is the possibility that one or more users of off channels not sufficiently spaced from Channels 15 and 16 could be located geographically much closer to the DF receiving station, thus stressing the dynamic range and off-channel rejection capabilities of the receiving equipment in attempting to receive weak Channel 15 and 16 signals in the presence of much stronger off-channel signals.

Finally, in some instances the DF receiving equipment may be sharing a site with other colocated high-power radar or other transmitting equipment, which, although far removed in frequency, could cause serious interference with DF reception by desensitizing receiver front ends.

3. ERROR ANALYSIS

3.1 Sources of Error in RDF Systems

We distinguish two general types of error sources: Those peculiar to the particular technique employed in the RDF operation, and those common to all techniques albeit they affect different techniques differently.

3.1.1 Common Error Sources

- Random background noise in the receiver
- Receiving site-effects, including:
  - Neighboring off-path reflectors (i.e., reflectors on one side or another of the azimuthal plane of the direction of incidence)
  - Counterpoise (if any) imbalance effect upon the patterns of individual receiving antennas
  - Antenna tower height effects
  - Stability of the plane of the antenna system under sway and torsional motion of antenna tower
- Cochannel and adjacent channel interference
- Receiver desensitization and capture by very strong off-channel signals
- Sea state effects, including wave shadowing, variation of polarization of radiated signal
- Receiving station reference misalignment
- Antenna pattern instability due to mechanical instability of supporting structure as well as of neighboring reflectors
- Receiving equipment drifts and departure from calibration

3.1.2 Error Sources Peculiar to Doppler RDF Technique

- Incomplete suppression of commutator-generated off-carrier sampling spectral zones
- Overlap of voice spectrum with the frequency of the induced DF sinusoidal Doppler frequency modulation

- Spurious modulation caused by asymmetry of the environment (e. g., ground plane, counterpoise, structural surroundings) relative to each of the commutated receiving antenna elements

- FM Demodulator random-noise threshold

3.1.3 Error Sources Peculiar to Adcock and Homer RDF Techniques

- Stability of antenna physical (for Adcock) and pattern orientation (for homer)

3.2 Analysis of Doppler RDF Systems

3.2.1 Random Noise Effects

Let the average power in the signal at the FM demodulator input be P_s watts, and the average noise power density be N_o watts/Hz at that point. If the effective predetection noise bandwidth is B_{ni} Hz, then the S/N ratio at the demodulator input is $P_s/N_o B_{ni}$. If this ratio exceeds 10dB, then the post-demodulation S/N ratio of the Doppler-induced DF sinewave is given by

$$(S/N)_{out} = \frac{P_s}{2N_o \beta_n} \cdot \frac{f_{d,max}^2}{f_m^2 + (\beta_n^2/12)}$$

$$\simeq \frac{P_s}{2N_o \beta_n} \cdot (f_{d,max}/f_m)^2, \text{ if } \beta_n^2/12 < f_m^2/10 \qquad (3.1)$$

where

$\beta_n \equiv$ effective noise bandwidth of an output bandpass filter centered at f_m Hz

and $f_{d,max}$ and f_m are, as defined in Section 2.3, the peak induced frequency deviation and f_m the frequency of the induced DF sinewave. The corresponding rms phase noise, σ_θ, that results in the phase measurement process that determines the azimuth of arrival of the incoming signal is given by

$$\sigma_\theta = \frac{40.5}{\sqrt{(S/N)_{out}}} \text{ degrees} \tag{3.2}$$

$$= \frac{40.5}{\sqrt{P_s/(2N_o \beta_n)}} \cdot \frac{f_m}{f_{d,max}} \text{ degrees} \tag{3.3}$$

$$= \frac{6.446}{\sqrt{P_s/(2N_o \beta_n)}} \cdot \frac{1}{r/\lambda_c} \text{ degrees.} \tag{3.4}$$

As stated earlier, this result holds as long as

$$P_s/(N_o B_{ni}) > 10. \tag{3.5}$$

Modulation wipe-off at the receiver, or inhibit at the transmitter, allows B_{ni} to be reduced to a minimum value of about

$$B_{ni} = 2f_m (1 + 2\pi r/\lambda_c) \tag{3.6}$$

where $2\pi r$ is the circumference of the circle of antennas. This minimum value of B_{ni} is well below the IF noise bandwidth for FM by voice when f_m is below the lowest speech frequency of interest, as in the Rohde & Schwarz and the Servo systems. In the Pilot system, the minimum B_{ni} is greater than or equal to the IF noise bandwidth for FM by voice.

If the f_m-Hz sinewave is extracted by means of a lowpass filter with upper cutoff frequency of $f_m + \beta_n/2$, then

$$(S/N)_{out} = \frac{P_s}{2(f_m + \beta_n/2)N_o} \cdot 3\left[\frac{f_{d,max}}{f_m + \beta_n/2}\right]^2 . \tag{3.7}$$

It is not clear from the available documents whether Equation (3.1) or Equation (3.7) more accurately applies to which of the three systems considered. A bandpass filter would of course be desirable in all cases, particularly in the Pilot system, but not really necessary in any of them, because the phase comparison (or detection) process can be made quite "linear", in which case the post-phase-detector filter could be made to suppress the effect of all noise (and voice spectrum) components that fall outside of a narrow band (the bandpass analog of the post-phase-detector lowpass filter bandwidth) centered around the frequency f_m.

Thus, with the filtering effect of the post-phase-detector lowpass (or equivalent data smoothing) filter taken into account, Equation (3.1) applies to each of the systems, with $\beta_n/2$ essentially equal to the noise bandwidth of the data output filter. The azimuth rms error is then given by Equations (3.2), (3.3) or (3.4).

Any drift in the phase characteristic of the filter that separates the Doppler-induced DF sinewave results in an error in the azimuth measurement.

3.2.2 Error Due to Overlap of Voice Spectrum With f_m

It is of course generally necessary to pre-filter the voice waveform prior to modulating the frequency of the radiated signal so that the residual spectral density of the voice is negligible within the β_n bandwidth around f_m. Modulation inhibit to aid the DF function would naturally eliminate the problem altogether. The voice-modulation wipe-off process in the Rohde & Schwarz system eliminates, or at least greatly reduces this problem.

The residual voice spectral components within $f_m \pm \beta_n/2$ can usually be treated as adding to the random noise spectral density and thus would be included in the value of N_o in the equations for $(S/N)_{out}$ and σ_θ given in Section 3.2.1.

3.2.3 Site Effects: Direct Plus Specular-Reflected Paths

The signal received from a distant transmitter in general consists of the direct signal plus reflections from a number of terrain features. In this analysis we consider only a single specular reflector to illustrate the method of computing the azimuth error introduced by multipath. This formulation, however, can be extended to the more general case of multiple reflectors, including scattering.

A signal ,

$$e_s(t) = E_s \cos\left[\omega_c t + \phi_c + \psi_v(t)\right] , \tag{3.8}$$

arriving from an azimuthal direction, θ_s, will be modified by the effect of the receiving antenna rotation into one expressible as :

$$e_s(t) = E_s \cos\left[\omega_c t + \delta \sin(\omega_m t + \theta_s) + \psi_v(t) + \phi_c\right] \tag{3.9}$$

where

ω_m is the angular "rotation" rate of the receiving antenna, $\cos(\omega_c t + \phi_c)$ represents the RF carrier and $\psi_v(t)$ denotes the frequency modulation by voice.

The single-reflector receiving station model is illustrated in Figure 3.2.1. The received RDF signal consisting of the contributions of a direct path and of a second specular-reflection path, can be expressed in the form :

$$\begin{aligned} e_{in}(t) = {} & E_s \cos\left[\omega_c t + \phi_{c1} + \delta \sin(\omega_m t + \theta_s) + \psi_v(t)\right] \\ & + aE_s \cos\left\{\omega_c (t - t_d) + \phi_{c2} + \delta \sin\left[\omega_m (t - t_d) + \theta_r\right]\right. \\ & \left. + \psi_v(t - t_d)\right\} \end{aligned} \tag{3.10}$$

where t_d represents the delay difference between the two paths, a represents the relative amplitude ratio of reflected signal to direct signal, and ϕ_{c1} and ϕ_{c2} are RF phase shifts.

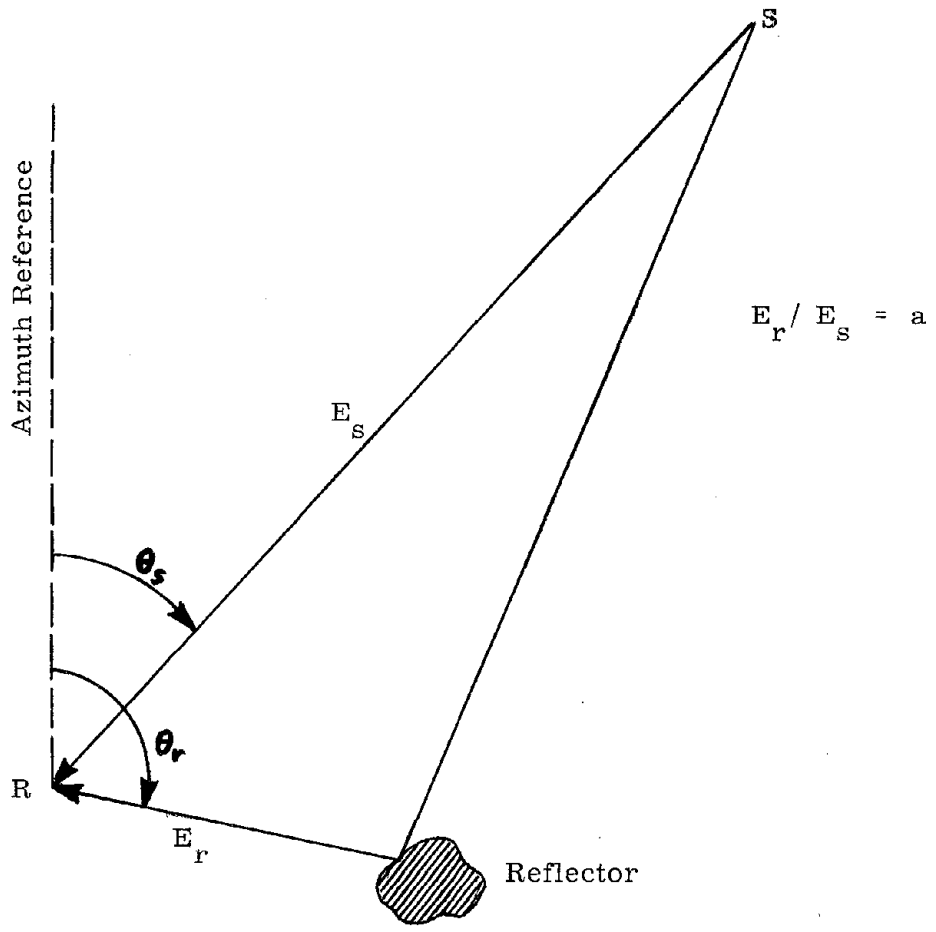

FIGURE 3.2.1 GEOMETRY OF DIRECT PLUS ONE SPECULAR-REFLECTED PATHS

This sum can be expressed in resultant form as :

$$e_{in}(t) = E_s A(t)\cos\left[\omega_c t + \phi_{c1} + \delta \sin(\omega_m t + \theta_s) + \psi_v(t) + \varphi(t)\right] \quad (3.11)$$

where

$$A(t) = \sqrt{1 + a^2 + 2a\cos\phi(t)} \quad (3.12)$$

$$\varphi(t) = \tan^{-1}\frac{a\sin\phi(t)}{1 + a\cos\phi(t)} \quad (3.13)$$

$$= \mathrm{Im}\left\{\sum_{n=1}^{\infty}\frac{(-a)^n}{n}e^{-jn\phi(t)}\right\}, \quad a^2 < 1 \quad (3.14)$$

and

$$\phi(t) = \delta\sin(\omega_m t + \theta_s) - \delta\sin\left[\omega_m(t - t_d) + \theta_r\right] + \omega_c t_d + \phi_{c1} - \phi_{c2} + \psi_v(t) - \psi_v(t - t_d). \quad (3.15)$$

The objective of this analysis is an expression for the error, θ_ε, added to θ_s by the presence of the reflected signal. Thus, we first express Equation (3.15) as :

$$\phi(t) = -\delta_d\sin(\omega_m t + \theta_s + \phi_d) + \Delta\phi_c + \Delta\psi_v(t) \quad (3.16)$$

where we have set

$$\delta_d = 2\delta\sin(\omega_m t_d + \theta_s - \theta_r)/2 \quad (3.17)$$

$$\phi_d = (\omega_m t_d - \theta_s + \theta_r - \pi)/2 \quad (3.18)$$

$$\Delta\phi_c = \omega_c t_d + \phi_{c1} - \phi_{c2} \quad (3.19)$$

and

$$\Delta\psi_v(t) = \psi_v(t) - \psi_v(t - t_d) \quad . \quad (3.20)$$

Next, we substitute from Equation (3.16) into Equation (3.14) to express the nth term under the summation sign in the form :

$$e^{-jn\,\phi(t)} = e^{-jn\Delta\phi_c} \cdot e^{-jn\,\Delta\psi_v(t)} \cdot e^{jn\,\delta_d \sin(\omega_m t + \theta_s + \phi_d)}$$

$$= e^{-jn\Delta\phi_c} \cdot e^{-jn\,\Delta\psi_v(t)} \sum_{k=-\infty}^{\infty} J_k(n\,\delta_d) e^{jk(\omega_m t + \theta_s + \phi_d)} \cdot \qquad (3.21)$$

If we now observe that only the $k = \pm 1$ terms are of interest here, we have:

$$\left\{ \omega_m \text{ component of } e^{-jn\phi(t)} \right\}$$
$$= 2jJ_1(n\delta_d) e^{-jn\Delta\phi_c} \cdot e^{-jn\Delta\psi_v(t)} \sin(\omega_m t + \theta_s + \phi_d) \cdot \qquad (3.22)$$

This expression can be simplified by noting that :

$$\left| \Delta\psi_v(t) \right| \approx t_d \left| \dot{\psi}_v(t) \right| \leq t_d \times 5 \times 10^3$$

so that $nt_d \times 5 \times 10^3 \leq 1/10$ for $t_d \leq 2 \times 10^{-6}$ sec and $n \leq 10$

and, that in addition, $a^{10}/10 < 0.035$ for $a \leq 0.9$.

Therefore, for all cases of practical interest, we can set $\exp\left[-jn\Delta\psi_v(t)\right] \approx 1$, and write :

$$\left\{ \omega_m \text{ component of } \varphi(t) \right\} \approx 2 \left[\sum_{n=1}^{10} \frac{(-a)^n}{n} J_1(n\,\delta_d) \cos n\,\Delta\phi_c \right] \cdot$$
$$\times \sin(\omega_m t + \theta_s + \phi_d) \cdot \qquad (3.23)$$

Accordingly, the ω_m component in the instantaneous phase of $e_{in}(t)$, Eq. (3.11), is given by :

$$\delta \left[\sin(\omega_m t + \theta_s) + (b/\delta) \sin(\omega_m t + \theta_s + \phi_d) \right] \qquad (3.24)$$

where

$$b \approx 2\sum_{n=1}^{10} \frac{(-a)^n}{n} J_1(n\delta_d)\cos n\Delta\phi_c \tag{3.25}$$

whence the azimuth error caused by the presence of the reflected path is given by

$$\theta_\varepsilon = \tan^{-1} \frac{b \sin \phi_d}{\delta + b \cos \phi_d} . \tag{3.26}$$

The significance of this azimuth error expression will now be brought out under certain important special conditions.

First, since $\omega_m t_d$ is extremely small in all case of practical interest, the expression for ϕ_d, Eq. (3.18), can be rewritten as:

$$\phi_d \approx (\theta_r - \theta_s - \pi)/2. \tag{3.27}$$

Similarly, $\omega_m t_d$ can be considered negligible in the expression for δ_d, Equation (3.17). The delay difference, t_d, between paths is therefore retained in the expression for θ_ε only in the phase difference, $\Delta\phi_c$, between RF carriers. The remainder, $\phi_{c1} - \phi_{c2}$, , is characteristic of the electromagnetic properties of the reflector. The reflector is also represented, of course, by the RF amplitude ratio, $\underline{a}$.

In almost all cases of practical interest $a \lesssim 0.2$, and hence b is closely approximated by

$$b \approx -2aJ_1(\delta_d)\cos \Delta\phi_c. \tag{3.28}$$

Thus, for small values of $\underline{a}$,

$$|b|_{max} \approx 2a\,|J_1(\delta_d)|_{max} \approx 1.2\,a \tag{3.29}$$

and

$$|\theta_\varepsilon|_{max} \approx 1.2\ a/\delta \text{ if } \delta >> |b|. \tag{3.30}$$

For $\delta \sim |b|$,

$$\theta_\varepsilon \approx \tan^{-1} \frac{\sin \phi_d}{1 + \cos \phi_d} = \phi_d/2, \quad b > 0 \tag{3.31a}$$

$$\approx \tan^{-1} \frac{\sin \phi_d}{1 - \cos \phi_d} = \pi/2 - \phi_d/2, \quad b < 0. \tag{3.31b}$$

For $\delta >> |b|$

$$\theta_\varepsilon \approx (b/\delta) \sin \phi_d \, . \tag{3.32}$$

The above results can be applied directly to the three Doppler RDF systems listed in Table 2.1. From the values of δ listed in Table 2.1, and in view of the cos $\Delta\phi_c$ factor in the expression for b, we conclude that:

- Equation (3.32) applies generally to the Rohde & Schwarz and the Servo systems.
- Equations (3.31) apply more typically to the Pilot system.

In order to compare the Rohde & Schwarz and the Servo systems, we first note that $J_1(\delta) \sim (2/\pi\delta)^{1/2}$ for large δ. Therefore, for large δ, and under worst-case conditions,

$$|\theta_\varepsilon| \propto \delta^{-3/2}. \tag{3.33}$$

Accordingly, under otherwise identical conditions, the ratio of θ_ε for R & S to θ_ε for S is given by

$$\theta_{\varepsilon,\,R\&S} / \theta_{\varepsilon,\,S} \approx \left(\delta_S/\delta_{R\&S}\right)^{3/2} \approx (0.523)^{3/2} = 0.378 \, . \tag{3.34}$$

For a = 0.2, Eq. (3.30) gives

$$|\theta_\varepsilon|_{max} = 2.44 \times 10^{-2} \text{ rad} = 1.40 \text{ degrees for R \& S}$$
$$= 4.66 \times 10^{-2} \text{ rad} = 2.67 \text{ degrees for S.}$$

This maximum error for S is seen to be 1.91 times the corresponding maximum error for R & S, where 1.91 is recognized to be the ratio of δ for R & S to that for S.

In the case of the Pilot system, it is first interesting to note from Eq. (3.26) that in situations where $\delta << |b|$,

$$\theta_\varepsilon \approx \phi_d \quad \text{if} \quad b > 0 \tag{3.35a}$$
$$\approx \pi - \phi_d \quad \text{if} \quad b < 0. \tag{3.35b}$$

This, in combination with Equations (3.31), suggests that worst-case errors for the Pilot system will range between the values given by Eqs. (3.5) when the Pilot receiving system is situated near a large reflector, and the values given by Equations (3.31) when the reflector is of more moderate (and typical) dimensions.

3.2.4 Site Effects: Direct Plus Two or More Specular-Reflected Paths

We consider first, for illustration, two specularly reflected additions to the direct-path signal, characterized by amplitude ratios a_1 and a_2 relative to the direct signal, and arriving at the receiving antenna system from azimuthal directions θ_{r1} and θ_{r2}. To simplify the computation, we restrict the analyzis to the more likely situation in which a_1 and a_2 are both in the order of 0.2 or less. The resultant of all three signals can then be expressed in the form of Equation (3.11) with

$$\varphi(t) \approx a_1 \sin \phi_1(t) + a_2 \sin \phi_2(t) \tag{3.36}$$

where $\phi_1(t)$ and $\phi_2(t)$ are each given by Equations (3.16) with corresponding subscripts added, and δ_{d1}, δ_{d2}, ϕ_{d1}, ϕ_{d2}, $\cos(\Delta\phi_c)_1$ and $\cos(\Delta\phi_c)_2$

are given by Equations (3.17), (3.18) and (3.19) with corresponding subscripts added. The voice modulation, if present, can be neglected for the purposes of this analysis for the reasons given in Section 3.2.3 .

Thus, we can readily show that under the above conditions, and for $\delta >> |b_n|, n = 1, 2,$

$$\theta_\varepsilon \approx (b_1/\delta) \sin \phi_{d1} + (b_2/\delta) \sin \phi_{d2} \tag{3.37}$$

where the various guantities are given by

$$b_n \approx -2a_n J_1(\delta_{dn}) \cos (\Delta\phi_c)_n \quad , n = 1, 2 \tag{3.38}$$

$$\phi_{dn} \approx (\theta_{rn} - \theta_s - \pi)/2 \quad , \quad n = 1, 2 \tag{3.39}$$

$$\delta_{dn} \approx 2\delta \sin \left[(\theta_s - \theta_{rn})/2 \right], \quad n = 1, 2 \tag{3.40}$$

and

$$(\Delta\phi_c)_n = \omega_c t_{dn} + \phi_{c1n} - \phi_{c2n}, \quad n = 1, 2. \tag{3.41}$$

The above results for two off-azimuth reflected signals can be generalized to more than two such signals under the condition that the relative amplitude ratios, a_n, are all small, and the resultant of the extraneous paths remains smaller than the direct-path signal almost all of the time. The same holds for one or more diffuse reflections, where a diffuse-reflected signal can be represented as the sum of a large number of differential components. In each of these generalizations, an rms value, σ_θ, would be calculated for the randomly distributed error, θ_ε. In the case of an off-azimuth diffuse reflector, the azimuth error consists of a bias-type error component that corresponds to an "equivalent" specular reflector, plus a randomly distributed component most conveniently represented by an rms value.

3.2.5 General Observations Regarding Errors Caused by Off-Azimuth Reflectors

Examination of the expressions for azimuth error, Equations (3.32) and (3.37) brings out the following facts:

a) The error is a function of the azimuth difference, $\theta_s - \theta_r$, between the direct path and each of the reflected paths.

b) The error is a function of the cosine of the RF carrier phase difference, $\Delta\phi_c$, of each reflected path relative to the direct path. The constituents of $\Delta\phi_c$ are essentially deterministic, not random.

c) The error is a function of the amplitude ratio, $\underline{a}$, of each reflected path relative to the direct path.

The above observations can be utilized to prepare charts for close determination of azimuth error for RDF at a particular, fixed receiving site. Such sites normally cover specifiable azimuth-angular sectors and have identifiable off-azimuth reflectors whose reflective characteristics can be measured. Thus, the parameters cited under a), b) and c) above can all be predetermined closely as a function of θ_s over the coverage sector and error charts prepared with θ_s as the independent variable. It is quite reasonable to expect that the values of the above parameters would not change very materially over the range of a small uncertainty in the measured value of θ_s. Thus, the "erroneous" value of θ_s just measured can be used to obtain a good estimate of θ_ε. Subtraction of this estimate of θ_ε from θ_s should yield an improved reading of θ_s. If desired, further iterations can be made using progressively improved readings on θ_s to reduce the θ_ε error below an acceptable tolerance level.

The expression in Equation (3.37) suggests another method for reducing the error due to an off-azimuth reflector; namely, the introduction

of another "balancing" reflector. The characteristics of such an added reflector can be adjusted empirically until the measured error falls below some desired tolerance level at least for particular preferred azimuth sectors.

3.2.6 Co-channel and Off-channel Interference

Co-channel and off-channel interference can affect the RDF reception in the following ways:

a) A very strong interfering signal of amplitude E_i and arbitrary frequency at the receiver input, which drives the front end into saturation, causes the desired signal level at the IF input to drop from AE_s to $(E_{lim}/2E_i)E_s$, where A is the linear amplification gain of the front-end-to-IF input stages, and E_{lim} is the output level of these stages at saturation. Thus, if $E_{lim}/E_i = 1/10$, for illustration, then the desired signal amplitude will drop from E_s at the front-end input to $E_s/20$ at the IF input. This is called "desensitization" and will cause serious degradation of signal relative to cochannel noise, regardless of whether the receiver frequency selectivity is or is not sufficient to reject the interfering signal. In addition, nonlinear operation of the front end gives rise to spurious by-products involving all signals present at the input without regard to their frequencies. Some of these by-products may indeed fall within the desired signal bandwidth and cause severe interference with the RDF function.

b) Interfering signals passed by the IF along with the desired signal will either completely capture the FM demodulator and thus suppress the desired signal, or will cause an error that can be described by an expression similar to that in Equation (3.32) for a single interfering signal (and Equations (3.37) for two interfering signals), except that now $\Delta\phi_c$ includes the term $\omega_d t$, where ω_d is the carrier frequency difference

between the desired signal and the interfering signal. Thus, if the desired signal captures theFM demodulator, the effect of the interference will be suppressed if $\omega_d/2\pi$ falls outside of the effective noise bandwidth of β_n centered about f_m.

c) Underlying the above is the effect of the receiving antenna commutation process which results in a spectrum such as is illustrated in Figure 2.3.4 for each input signal present. Thus, the "cochannel" interference may actually result from an off-center spectral zone of the undesired signal falling within the desired band. This problem can be reduced or eliminated only by proper design of the antenna commutation "blending function."

3.2.7 Effects of Sea State

Rough sea state, with consequent wave shadowing and swaying of the transmitting antenna over wide angles,can cause

a) Wide fluctuations in received signal level, and hence in the S/N ratio

b) Wide deviations of received signal polarization both relative to the RDF receiving antenna and the reflecting surfaces (or structures) causing the multipath.

The potentially most detrimental consequence of b) is the wide fluctuation in amplitude ratios of the received (desired and undesired-path) signals, and the possibility, with an elevated receiving antenna, of the off-azimuth signal (or signals) emerging close in amplitude to, or exceeding,the desired correct-azimuth signal (the latter may be the resultant of direct plus intervening-surface-reflected paths). This and the corresponding fluctuations in $(\Delta\phi_c)$ may also complicate the successful implementation of the error-reduction measures discussed in Section 3.2.5.

3.3 Analysis of Adcock RDF System

The Adcock RDF technique operates on a form of "paired-antenna" interferometer principles. We shall address here only the effect of multipath upon azimuth-measurement performance. The effect of random noise and interference depend too much on receiver functional structure and design characteristics that have not been available for this analysis.

Consider two antennas spaced a distance, L, apart. With reference to Figure 3.3.1, antenna A_1 receives a resultant carrier represented by

$$e_{A1}(t) = \cos \omega_c t + a \cos \omega_c (t - t_d) . \tag{3.42}$$

Antenna A_2 receives

$$e_{A2}(t) = \cos\left[\omega_c t + 2\pi (L/\lambda_c)\cos \theta_s\right] + a \cos\left[\omega_c(t-t_d) + 2\pi(L/\lambda_c) \cos \theta_r\right] . \tag{3.43}$$

If we assume that $a \leq 0.2$, then the phase difference between $e_{A2}(t)$ and $e_{A1}(t)$ can be approximated by

$$\phi_{A1} - \phi_{A2} = 2\pi(L/\lambda_c)\cos \theta_s + (\varphi_2 - \varphi_1) \tag{3.44}$$

where

$$\begin{aligned} \varphi_2 - \varphi_1 &\approx - a \sin\left[\omega_c t_d + 2\pi (L/\lambda_c) \cos (\theta_s - \theta_r) + a \sin \omega_c t_d\right] \\ &\approx - 2a \sin\left[\pi (L/\lambda_c)\cos(\theta_s - \theta_r)\right] \\ &\quad \times \cos\left[\omega_c t_d + \pi(L/\lambda_c) \cos (\theta_s - \theta_r)\right] \end{aligned} \tag{3.45}$$

Thus, the error in measured RF phase difference has a maximum value approximated by

$$| \varphi_2 - \varphi_1 |_{max} \approx 2a .$$

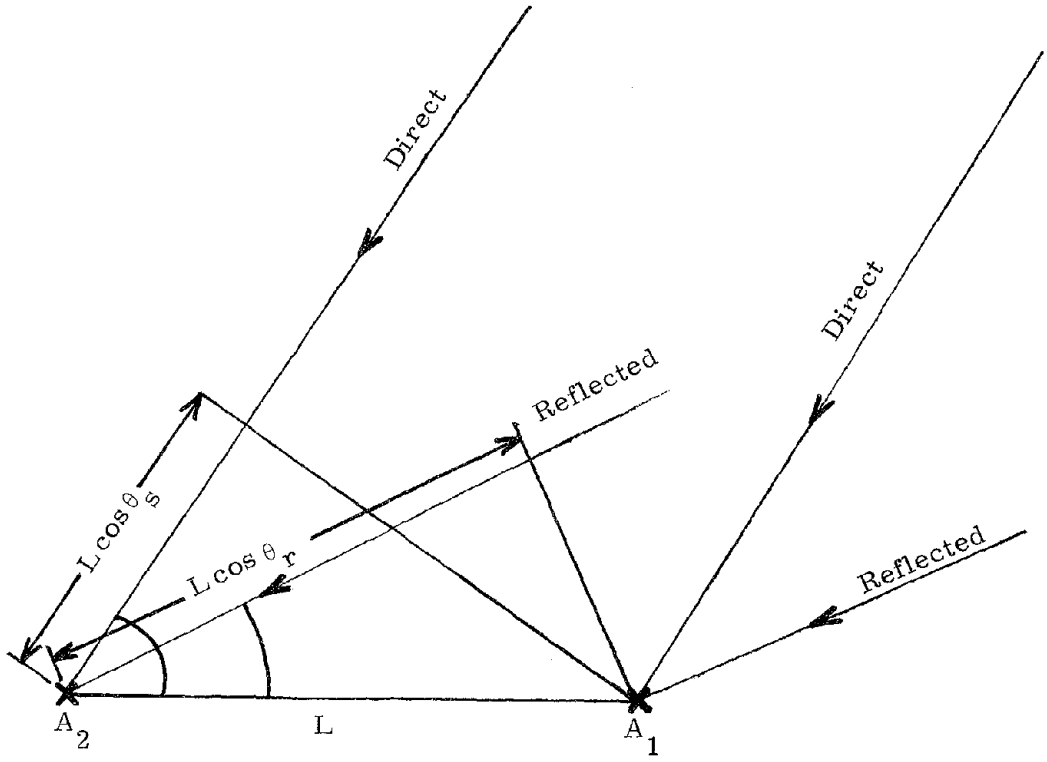

FIGURE 3.3.1 GEOMETRY OF A PAIR OF ANTENNAS IN AN ADCOCK RDF SYSTEM, WITH INCIDENT DIRECT AND REFLECTED RAYS

The corresponding error in computed cos θ_s is:

$$(\cos\theta_s)_\varepsilon\big|_{max} \approx \frac{1}{2\pi(L/\lambda_c)}\left|\varphi_2 - \varphi_1\right|_{max}$$

$$\approx \frac{a/\sqrt{2}}{\pi(L/\lambda_c)} = 2\sqrt{2}\,a/\pi \quad \text{for } L = \lambda_c/4 \quad . \qquad (3.46)$$

But

$$\Delta\cos\theta_s \approx -\sin\theta_s\,\Delta\theta_s \,.$$

Therefore,

$$\theta_\varepsilon \approx \frac{-1}{\sin\theta_s}(\cos\theta_{s_\varepsilon})$$

and

$$|\theta_\varepsilon|_{max} \approx 0.900\,a/\sin\theta_s \qquad (3.47)$$

$$\approx \frac{0.180}{\sin\theta_s} \qquad \text{for } a = 0.2 \,.$$

This error ranges from 10.32 degrees for $\theta_s = \pi/2$ to a value that becomes unbounded as $\theta_s \rightarrow 0$ or π .

For comparison of the Adcock error with the error in Doppler DF, we have for $a \leq 0.2$ and large δ :

$$|\theta_\varepsilon,\ \text{Adcock}\ |/|\theta_\varepsilon,\ \text{Doppler}\ | \approx \frac{\sqrt{2}}{\pi}\cdot\frac{\delta}{|J_1(\delta)|}\cdot\frac{1}{\sin\theta_s}$$

$$\approx \frac{0.564}{\sin\theta_s}\,\delta^{3/2} \qquad (3.48)$$

$$\approx \frac{6.60}{\sin\theta_s} \quad \text{for} \quad \delta = 5.15 \quad (S)$$

$$\approx \frac{17.44}{\sin\theta_s} \quad \text{for} \quad \delta = 9.85 \quad (R\&S) \,.$$

3.4 Analysis of Homer System

The antenna patterns portrayed in Figure 2.5.2 for the D & M Homer system are those of cardioids in the horizontal plane, one described by

$$P_o(\theta) = 1 - \cos\theta \tag{3.49}$$

the other by

$$P_\pi(\theta) = 1 + \cos\theta . \tag{3.50}$$

If only the direct-path signal is present, the "homing" course is set by orienting the navigating craft so that

$$E_s P_o(\theta) = E_s P_\pi(\theta) \tag{3.51a}$$

i.e., so that

$$\theta = \pi/2. \tag{3.51b}$$

Now consider the situation in which the signal arrives over one off-azimuth reflected path, in addition to the direct path. Let θ_d and $\theta_d + \theta_r$ denote the angles of arrival, relative to the reference angle of the above expressions for the antenna polar patterns, of the direct and the reflected incident signals. If the amplitudes of the signals, before weighting by the antenna patterns, are E_s and aE_s, $a < 1$, then one of the antennas delivers

$$E_s P_o(\theta_d)\cos\omega_c t + aE_s P_o(\theta_d + \theta_r)\cos\left[\omega_c(t-t_d) + \phi_c\right] \tag{3.52}$$

and the other delivers

$$E_s P_\pi(\theta_d)\cos\omega_c t + aE_s P_\pi(\theta_d + \theta_r)\cos\left[\omega_c(t-t_d) + \phi_c\right] . \tag{3.53}$$

The receiving unit extracts the envelope of each of the above resultants. A coherent product detector would yield an output proportional to

$$V_{out,1} = P_o(\theta_d) + aP_o(\theta_d + \theta_r)\cos(\omega_c t_d + \phi_c) \tag{3.54}$$

corresponding to (3.52), and

$$V_{out,2} = P_{\pi}(\theta_d) + a\,P_{\pi}(\theta_d + \theta_r)\cos(\omega_c t_d + \phi_c) \qquad (3.55)$$

corresponding to (3.53). The corresponding outputs of an envelope detector are approximated by (3.54) and (3.55) on the assumption that the amplitude ratio of weaker-to-stronger signal in each of (3.52) and (3.53) is in the order of 0.2 or less.

Setting the course of the navigating craft or orienting the "boresight" of the system so that (3.54) and (3.55) are equal, yields

$$P_o(\theta_d) - P_{\pi}(\theta_d) + a\cos(\omega_c t_d + \phi_c)\,P_o(\theta_d + \theta_r) - P_{\pi}(\theta_d + \theta_r) = 0. \qquad (3.56)$$

Substitution from Equations (3.49) and (3.50) into (3.56) yields

$$\cos\theta_d + a\cos(\omega_c t_d + \phi_c)\cos(\theta_d + \theta_r) = 0. \qquad (3.57)$$

Now, as stated in Equation (3.51), the correct value for θ_d is $\pi/2$. Let the directional error caused by the reflected path be θ_ε; i. e., in Equation (3.57), set

$$\theta_d = \pi/2 + \theta_\varepsilon \quad . \qquad (3.58)$$

This yields

$$\tan\theta_\varepsilon = \frac{-a\cos(\omega_c t_d + \phi_c)\sin\theta_r}{1 + a\cos(\omega_c t_d + \phi_c)\cos\theta_r} \quad . \qquad (3.59)$$

This expression is readily recognized to be of the same form as the expression in Equation (3.26) for Doppler DF systems, which facilitates the comparison between the two types of D. F. systems. For example, for $a \leq 0.2$ and $\delta >> |b|$,

$$\begin{aligned} |\theta_{\varepsilon\ \text{homer}}/\theta_{\varepsilon,\ \text{Doppler}}| &\approx \frac{\delta}{2|J_1(\delta)|} \\ &\approx 0.627\delta^{3/2} \qquad (3.60) \\ &\approx 7.33 \quad \text{for} \quad = 5.15 \quad \text{(S)} \\ &\approx 19.38 \quad \text{for} \quad = 9.85 \quad \text{(R\&S)} \end{aligned}$$

4. EXPERIMENTAL PROGRAM

4.1 Introduction

A series of tests were conducted to verify range of reception of the EPIRB signal by representative shore-based radio direction finders. In addition, range tests were conducted with homer equipped cutters and helicopters. Finally, on September 28, 1977, the complete set of equipment was demonstrated to personnel from Coast Guard Headquarters, the FCC, and NASA at the Point Allerton C.G. Station, Hull, Massachusetts.

Again, mention must be made of the limited scope of the tests described herein. The resources available permitted a demonstration of commercially available direction finders and homers, but did not allow a detailed performance evaluation or comparative evaluation of the equipment selected for the tests.

The following is a list of direction finding equipment utilized for the tests and demonstration:

(I) Pseudo-doppler type RDF

(1) Servo Corp of America Model 7010M - marine version of a unit in wide use in aeronautical applications

(2) Intech Inc. Model M360 - desgined for shipboard applications in the fishing industry and pleasure craft

(II) Adcock type RDF

Ocean Applied Research (OAR) Model ADFS-320 - designed for heavy duty industrial/military shipboard applications.

(III) Cutter installed Homer

(1) Dorne & Margolin Model DM SE47-7.

(2) Intech Inc. Model. (Not available.)

(IV) Helicopter installed homer

Dorne & Margolin Model DM SE47-2.

Salient characteristics of the DF units are presented in Table 4.1. Manufacturer's specifications are included as Appendix A.

TABLE 4-1 COMMERCIALLY AVAILABLE VHF-FM DIRECTION FINDERS

BRAND	SERVO CORP OF AMERICA	INTECH INC.	PILOT INSTRUMENT CORP.*	OCEAN APPLIED RESEARCH CORP.
MODEL	7010M-11	MARINER 360	804 RA-7	ADFS-320
TYPE	Wide Aperture Quasi Doppler	Small Aperture Doppler	Small Aperture Doppler	Adcock Array
SENSITIVITY	5μV/m	~5μV/m	5μV/m	1μV/m
ACCURACY				
Instrumental	±1°	±2°		
Overall	±3°		±5°	±3°
MEASUREMENT TIME	1/2, 1, 2 sec. Averaging Time (Operator Controlled)	<3 sec.	Continuous Reading	Continuous Reading
ANTENNA SYSTEM	16 dipoles on 3.14 m diameter	Four $\frac{\lambda}{4}$ elements on 8" diameter above ground plane of four 24" radials	Four $\frac{\lambda}{4}$ elements on 3" diameter above ground plane of four 18" radials	Dipole Adcock Array - 18" O.D.
DISPLAY	DIGITAL - 3 digit one degree increments	DIGITAL - 3 digit	MECHANICAL	CRT
PRICE	$27,000 $39,000 with remote	$2,200	$1,000	$4,000-$5,000
COMMENTS	System in wide use by FAA, Canadian Ministry of Transport, et al	System evaluated at USCG Electronics Research Center	System evaluated at USCG Electronics Research Center. Add on to existing transceiver	System evaluated at USCG Electronics Research Center

*This unit was not used in field tests.

4.2 Field Tests

4.2.1 Shore-Based RDF Tests at Winthrop Highlands, Massachusetts

The primary field site for this experiment was located at Winthrop Highlands, Massachusetts. The receiving site consisted of an open field about 20 feet above sea level, located on the shore line. The nearest reflecting obstacles were an apartment building and an FAA enroute radar installation, both approximately 1000 feet to the west of the test site. A Cortez 24 foot van with auxiliary power unit was used as an equipment shelter, and instrumented to measure and evaluate all test signals. The Servo Corp. antenna, consisting of a 10 foot diameter dipole array, was mounted on the roof of the equipment shelter using a 5 foot mast (Figures 4.1 and 4.2). This gave the antenna a total height of about 30 feet above sea level. The Intech and OAR antennas were erected using standard photographic tripods at heights of approximately 25 feet above sea level. The signal source used for the tests was a prototype EPIRB [1] which was capable of transmitting approximately 1 watt on channel 15 (156.750 MHz). The EPIRB was deployed in the water by a Coast Guard cutter at specific test sites which were adjacent to major buoys in the Boston Harbor area (Figure 4.3).

The received signal strength was measured as shown in Figure 4.4. The signal was received by a dipole mounted on the van roof. It was then amplified in a low noise preamp, further amplified and then converted to I.F. The IF signal at 30 MHz was displayed on a spectrum analyzer. A calibrated signal generator was used to provide a reference signal at the preamp input.

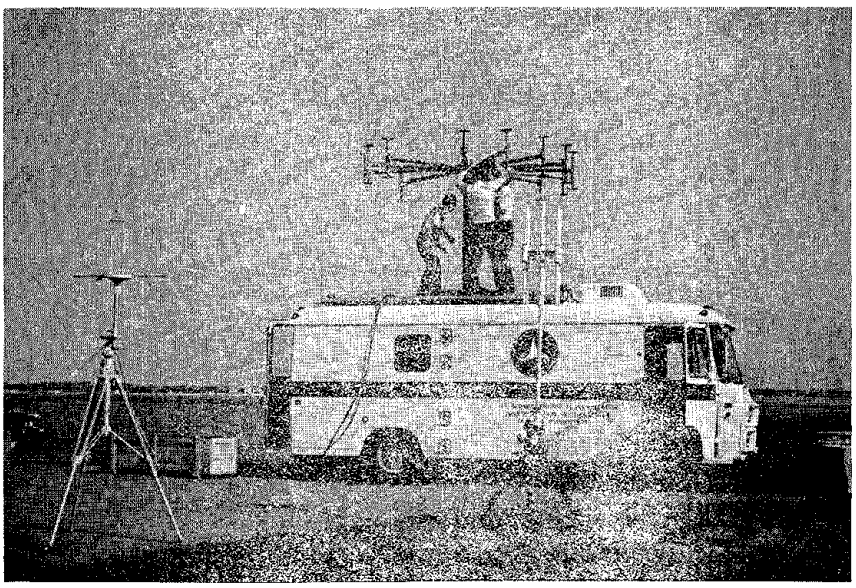

FIGURE 4.1 TEST SITE AT WINTHROP, MASSACHUSETTS

FIGURE 4.2 SERVO CORP. DF ANTENNA MOUNTED ON TEST VAN

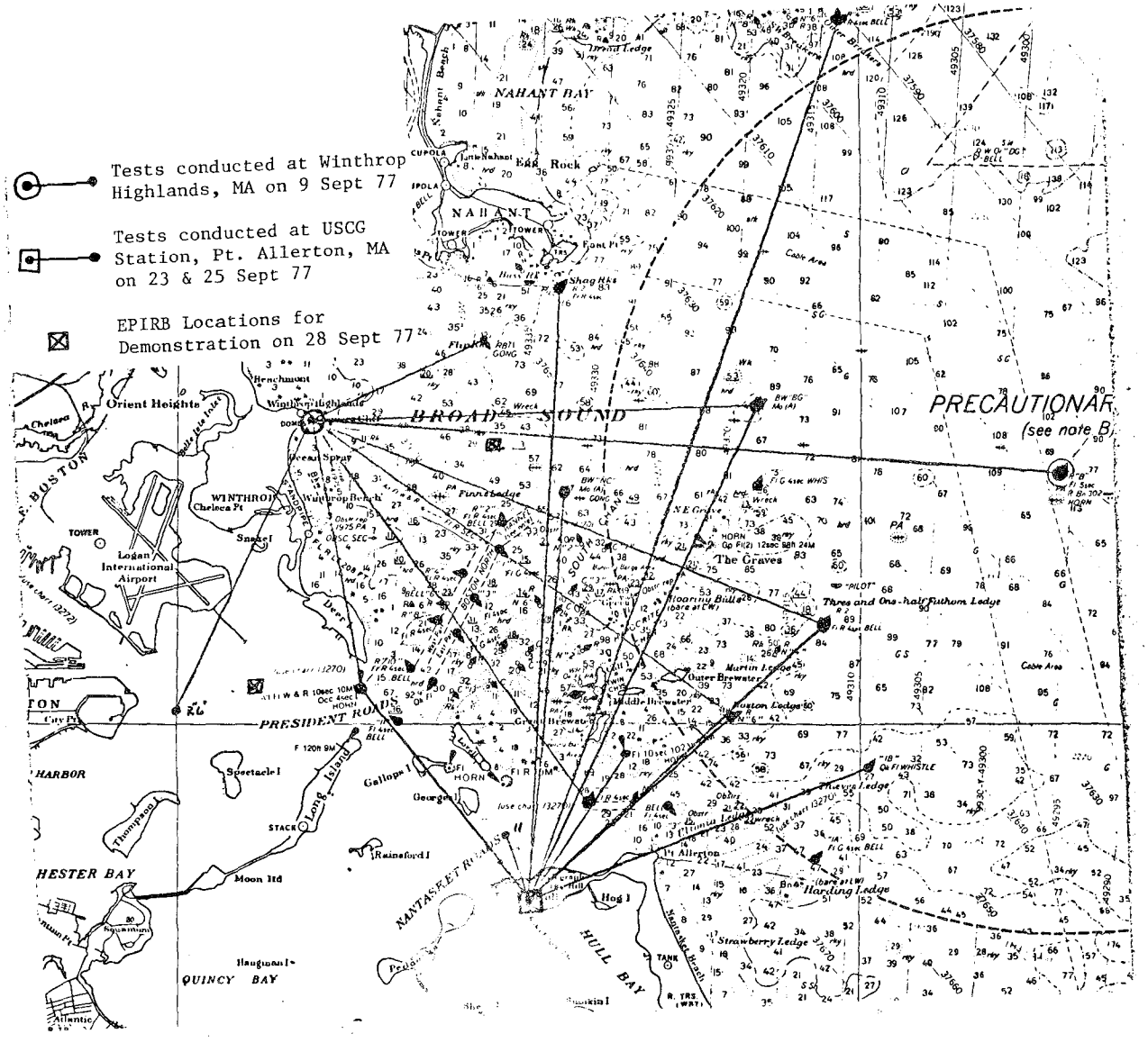

FIGURE 4.3. DIAGRAM OF Shore-Based DIRECTION FINDER TESTS

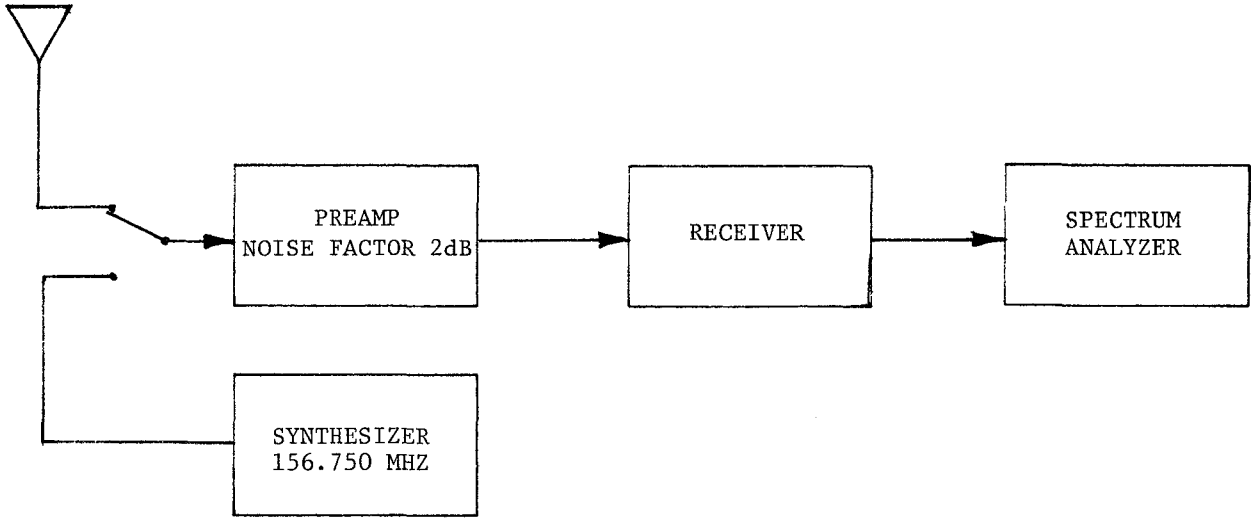

FIGURE 4.4 DIAGRAM OF SIGNAL STRENGTH MEASUREMENT SYSTEM

Figures 4.5 and 4.6 present typical shore-based DF performance. The plots present bearing accuracy as a function of range. Other than signal level, the main factors affecting the accuracy of the obtained bearings were range and land blockage. The effect of range can be seen in Figure 4.6, where bearing variation vs. distance is shown for the data points taken from Winthrop on Sept. 9. As was expected, the variation in readings increased as a function of range. At the eight nautical mile data point, variation had reached $\pm 5°$, which is about the limit of usability at this antenna height. Independently measured values of received signal power are noted at the lower ends of the variation bars in Figure 4.6 and indicate that $\pm 3°$ variation was observed at received signal strengths of approximately -100 dBm, whereas $\pm 5°$ variation was obtained at signal levels of -105 to -110 dBm. As a point of reference, a commercial FM receiver designed for maritime mobile service and fed from a Phelps-Dodge Model 1-5 dipole, produced a clear audio signal down to a measured signal level of -117 dBm. From this we infer that the Servo unit, which was designed for line of sight aeronautical applications with relatively strong signals, is not optimum in terms of sensitivity as procured for the Coast Guard application.

Although the other DF units tested showed somewhat greater sensitivity, these units lack the accuracy and relative immunity to reflections that the larger aperture Servo unit can furnish, given adequate signal levels. In any case, a major improvement in signal level would accompany increased antenna height. Figure 4.7 presents receiving antenna height as a function of range assuming the transmitting antenna is at surface level.[2] It can be seen for example that a range of 20 nmi could be expected with a receiving antenna height of approximately 260 feet.

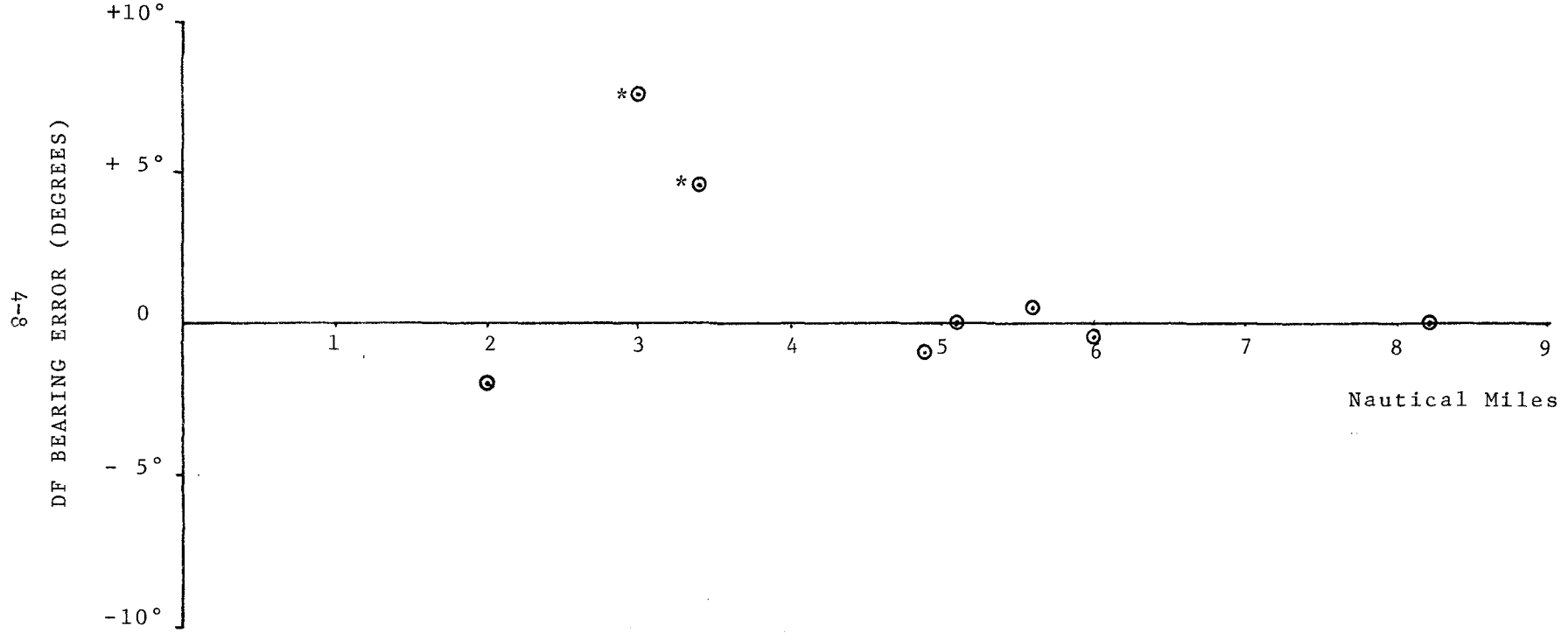

FIGURE 4.5 DF BEARING ERROR VS. RANGE IN NAUTICAL MILES - TYPICAL PERFORMANCE. (ASTERISKS DENOTE DATA POINTS TAKEN ON PATHS WITH SUBSTANTIAL LAND INTERVENTION)

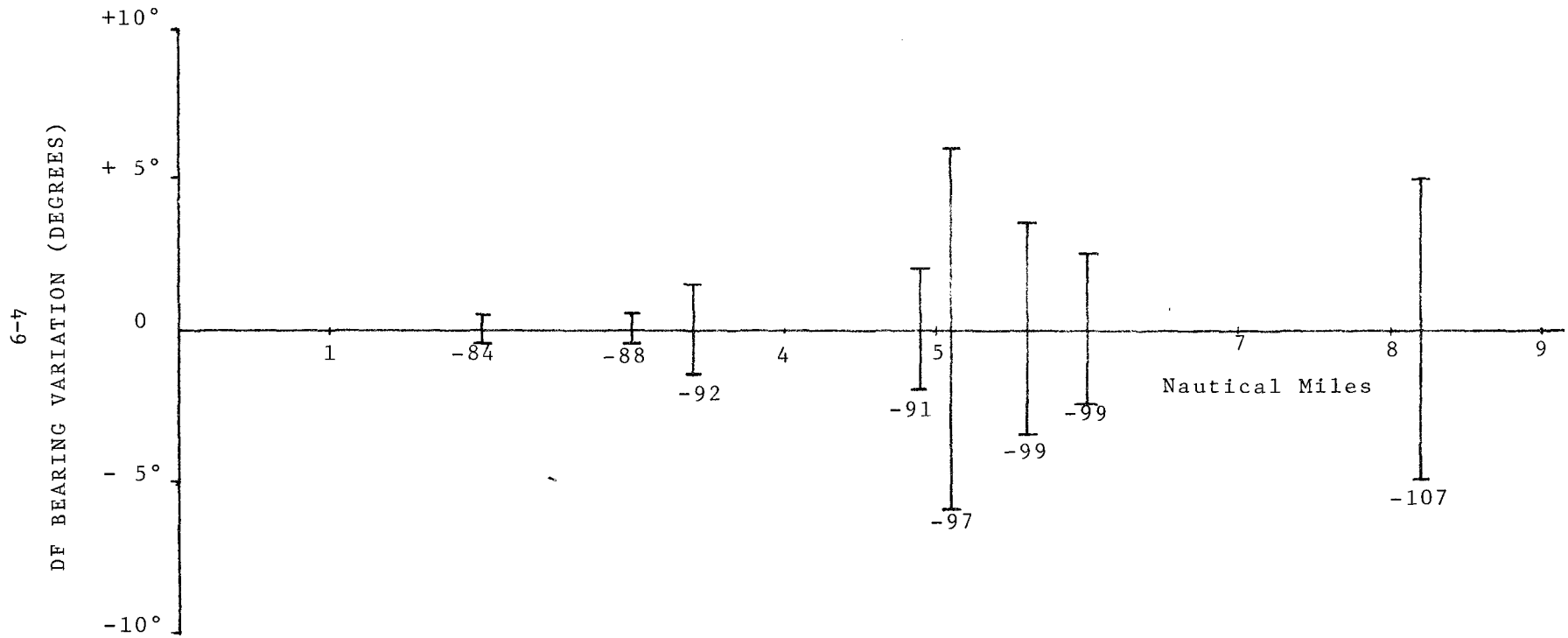

FIGURE 4.6 DF BEARING VARIATION VS. RANGE IN NAUTICAL MILES, TYPICAL PERFORMANCE - RECEIVED SIGNAL LEVEL IN dBm NOTED UNDER VARIATION BARS

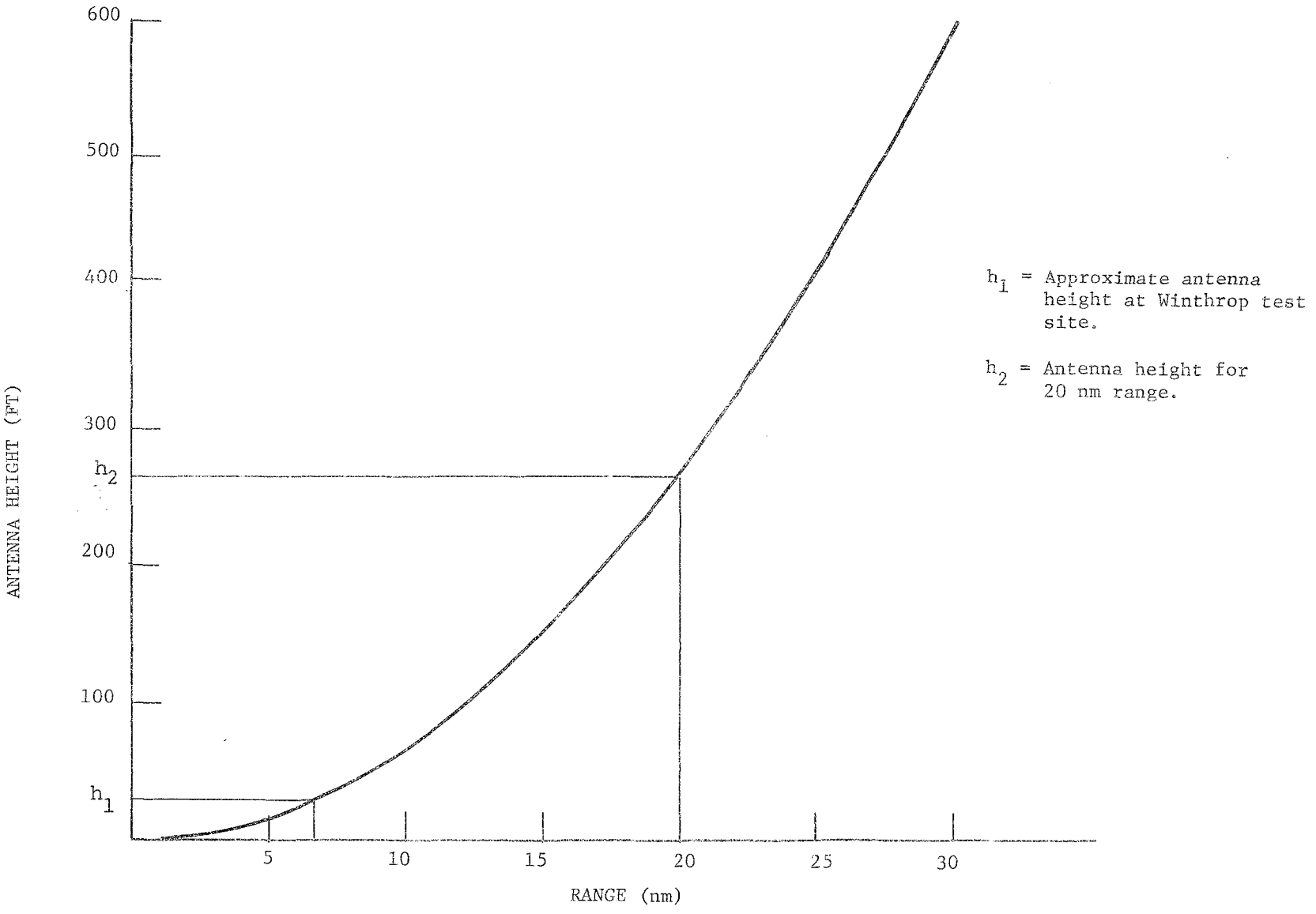

FIGURE 4.7 ANTENNA HEIGHT VS. RANGE FOR TRANSMITTING ANTENNA ON SURFACE

During the tests and demonstrations the digital displays of the Servo and Intech units were compared to the CRT display of the OAR. In the OAR CRT display the length of the bearing indicating vector is a function of the received signal level. This was judged to be a particularly advantageous feature for shore based installations with range or siting limitations, which would be operating on signals of widely differing levels. The vector length would allow the operator to establish a confidence level on the bearing. In addition, the display proved easier to interpret in situations where the observed bearing was exhibiting substantial fluctuation.

A feature which was available on the Servo unit but not evaluated was remoting capability. In some siting situations it may be advantageous to locate the DF antenna some distance from the station to take advantage of an existing tower or a nearby hill. In the Pt. Allerton site, the actual promontory from which the area takes its name is located approximately 1/2 mile from the station, but affords an excellent outlook on the ocean and higher elevation. The antenna of a DF unit with remoting capability such as the Servo 7010 could be located at the Pt. Allerton and be linked to the station via voice grade phone line.

Finally, the antenna and electronic components must be sufficiently rugged to withstand the environmental requirements of the shore based application. The Servo 7010M, having been designed to serve in operational aeronautical applications, was judged completely adequate in this respect. The OAR unit was quite rugged also, but the antenna of the Intech 360M appeared to lack the sturdiness required for the all-weather all-year service of a shore-based installation.

Thus each of the demonstrated DF units possessed features desirable for shore based applications, but no single unit encompassed all the features.

4.2.2 Tests Conducted with Homer Equipped Cutter

One Coast Guard 41' cutter was equipped with a Dorne and Margolin type DM SE47-7 VHF-FM homing direction finder. The antenna, consisting of dual whip antennas (Figure 4.8) was installed on the masthead and can be seen projecting above the flags in Figure 4.9. The prototype EPIRB was deployed in the water, at various sites. The EPIRB duty cycle was set to transmit on Channel 15 for a period of 10 seconds, followed by 20 seconds off time. The cutter helmsman thus received a left/right indication for a period of ten seconds every 30 seconds and was required to turn the cutter, attempting to center the homing indicator. There was no problem encountered in homing on this duty cycle in an open sea situation, and the cutter consistently homed directly to the EPIRB from ranges to 8 nautical miles. However, in situations where the cutter must deviate repeatedly from a direct course to the EPIRB to avoid islands and follow channels, the 10 second on time was considered inadequate. For this reason, a 15 second on time with a proportionately longer off time (30 sec) is presently being implemented as a possible improvement.

An additional experiment was conducted using two EPIRBs simultaneously deployed with duty cycles of 10 seconds on, 80 seconds off. Due to the long off time, the EPIRB transmissions did not overlap, and the helmsman was able to home on one successfully, turn it off, and then home on the remaining EPIRB. However, considerable attention was required to avoid confusing the two interleaved transmissions, and an automatic lock-on

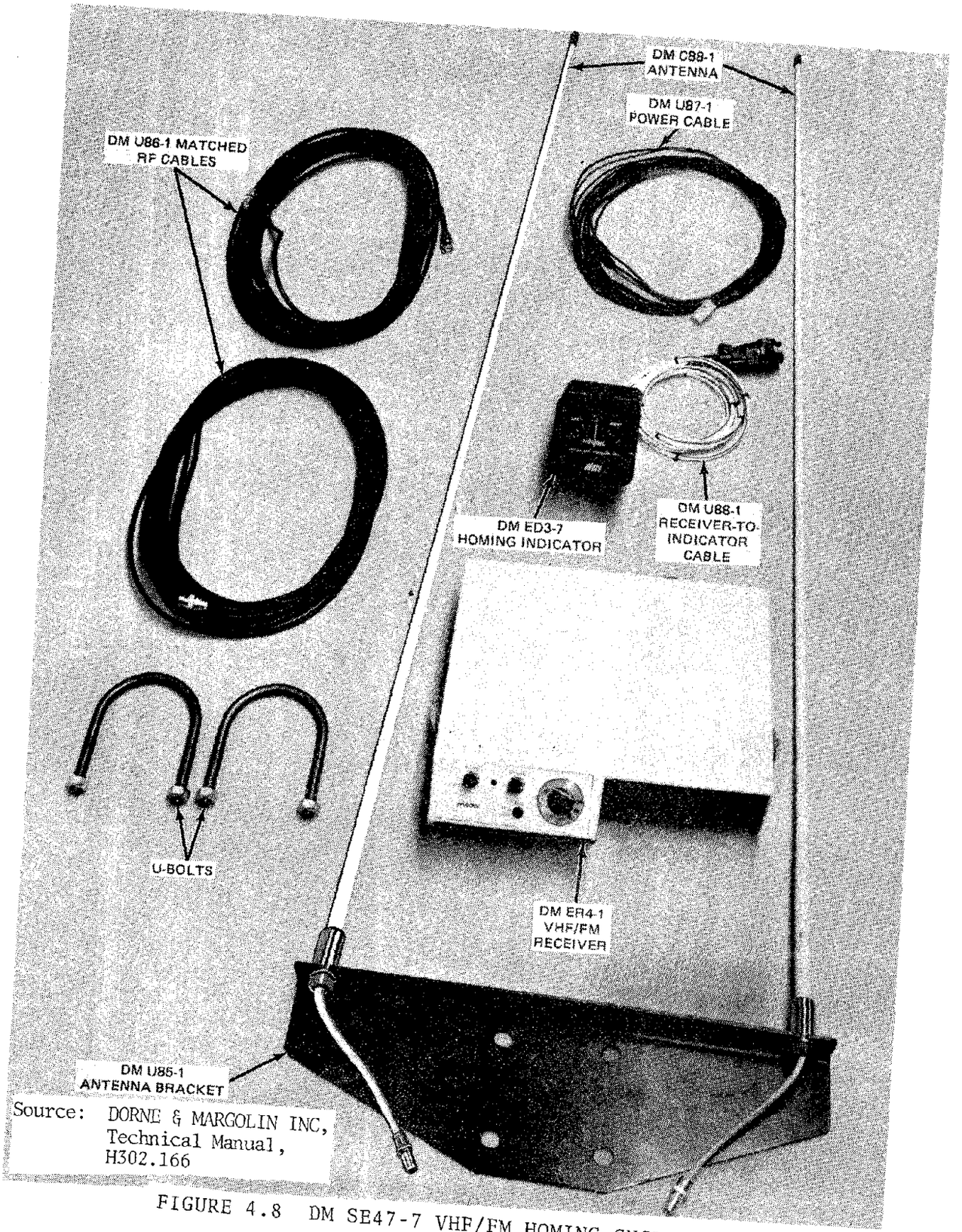

Source: DORNE & MARGOLIN INC, Technical Manual, H302.166

FIGURE 4.8 DM SE47-7 VHF/FM HOMING SYSTEM

feature in the homer, which could display a specific EPIRB identification, would lighten crew workload considerably in the multiple EPIRB operation. Also, the inadequacy of the 10 second on time was heightened by the necessity to wait 80 seconds for the next bearing.

As an additional comment, all homing experiments were conducted in relatively calm seas. It would be more difficult to attain similar results in heavy seas, where the cutter could not be safely turned to a bearing at the particular time that the EPIRB transmitted. In this situation, the capability of an RDF to furnish a bearing without the necessity of turning the cutter to the actual bearing would be of value.

4.2.3 Tests Conducted with Homer Equipped Helicopter

Tests were conducted with a Coast Guard Type HH-52 helicopter which was already equipped for homing operation in the VHF band.[3] This homer uses the helicopter's VHF transceiver. However, in the homing mode the unit uses two belly-mounted blade antennas together with an external antenna switch to provide a homing signal. The helicopter and the homer antenna installation are shown in Figures 4.10 and 4.11 respectively.

The helicopter, operating on the EPIRB signal, was able to home from a range of 18 nautical miles at an altitude of 500 feet. This range increased to 21 nmi at an altitude of 1000 feet. However, when the homing mode was disabled, and the EPIRB signal was received via the normal VHF-FM communications antenna instead of the belly mounted twin blade DF antenna, the EPIRB signal could be clearly heard at a range of 32 nmi at an altitude of 1000 feet. Subsequent discussion with the helicopter pilots indicated that it was normal to experience a substantial loss of sensitivity in the homing mode. This would indicate that a significant range improvement could be obtained with a relocation or replacement of the homer antenna with a higher gain device.

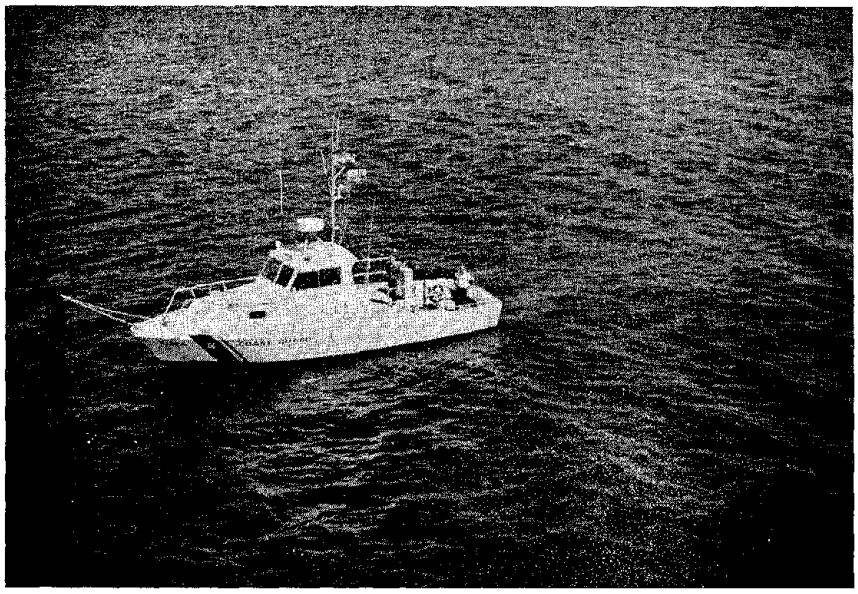

FIGURE 4.9 FORTY-ONE FOOT CUTTER WITH HOMER INSTALLED (HOMER ANTENNA CAN BE SEEN ABOVE FLAGS)

FIGURE 4.10 HH-52 HELICOPTER USED IN HOMING TESTS

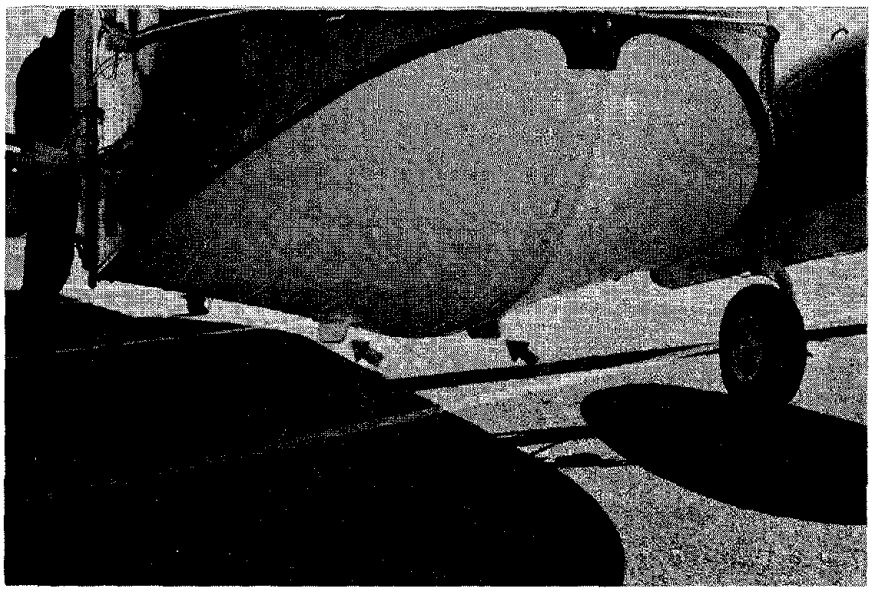

FIGURE 4.11 HOMER ANTENNA INSTALLATION ON HH-52 HELICOPTER (ARROWS INDICATE ANTENNA BLADES.)

A summary of the results of the tests described in Section 4.2 is presented in Table 4.2.

4.3 System Demonstration at USCG Station, Pt. Allerton, Massachusetts

4.3.1 Site Preparation

The receiving test site was moved to the roof of the Pt. Allerton Coast Guard Station, Hull, Massachusetts in preparation for a system demonstration to be performed for personnel from the Coast Guard, FCC, & NASA. The antennas were deployed as shown in Figures 4.12 and 4.13. Due to the presence of considerable land masses to the east and southeast of the station, which completely blocked line-of-sight paths from the ocean surface to the antenna locations, preliminary testing of DF reception from various azimuths was conducted. Two EPIRB test locations were selected which included significant close-in land blockage in the line of sight to the receiving antenna: 7.6 nmi on a bearing of 119°M and approximately the same distance on a bearing of 068°. No usable DF bearings were attained on either path. This contrasts with the Winthrop/LNB test point, a clear path of the same range, where bearings within $\pm 5°$ of measured bearing were obtained from each of the three DF test units. After this directionality was established further testing was restricted to the areas to the north and northeast of the station (Boston Harbor, Winthrop, Nahant areas) and results similar to the Winthrop results were attained.

To complete the preparations, the electronic bearing display equipment was installed in a large assembly room within the station.

4.3.2. System Demonstration

On September 28, 1977, the demonstration was performed. An EPIRB was deployed in the President Roads achorage area approximately 4 nmi from the Pt. Allerton Station. Immediately upon receipt of the signal by the Pt. Allerton radio watch, the station dispatched a 41 foot cutter and requested a bearing from the DF room. This bearing was then transmitted to the cutter,

TABLE 4.2 MAXIMUM RANGES ACHIEVED IN DF & HOMING TESTS

TEST	ANTENNA HEIGHT OR ALTITUDE ASL	MAXIMUM RANGE FOR +5° ACCURACY
SHORE BASED DF	30'	8-12 nmi
HOMER MOUNTED ON 41' CUTTER	15'	8 nmi
HOMER EQUIPPED HH-52 HELICOPTER	500' 1000'	18 nmi 21 nmi

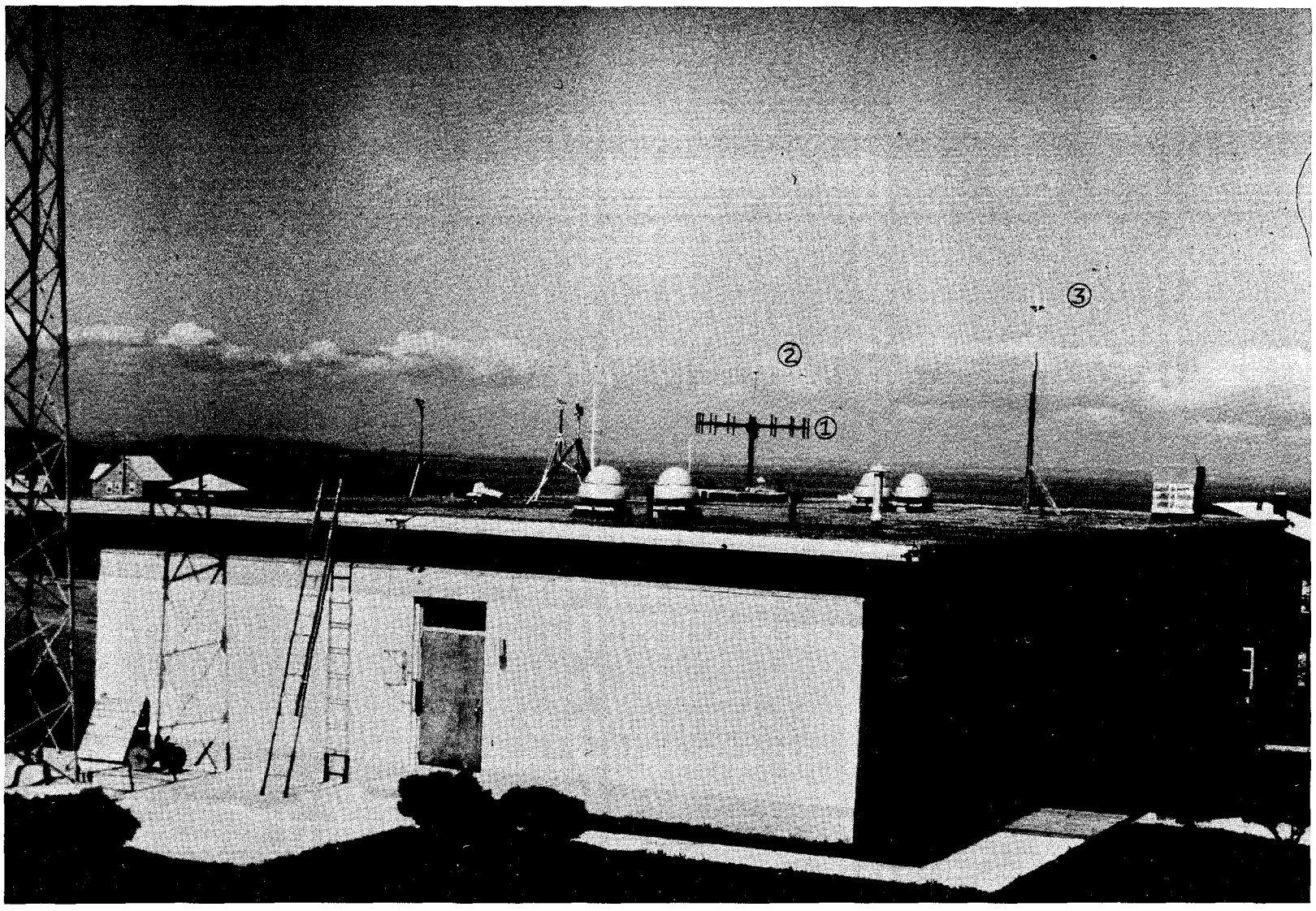

FIGURE 4.12 DF ANTENNAS DEPLOYED ON ROOF OF POINT ALLERTON STATION
(1) SERVO; (2) INTECH; (3) OAR

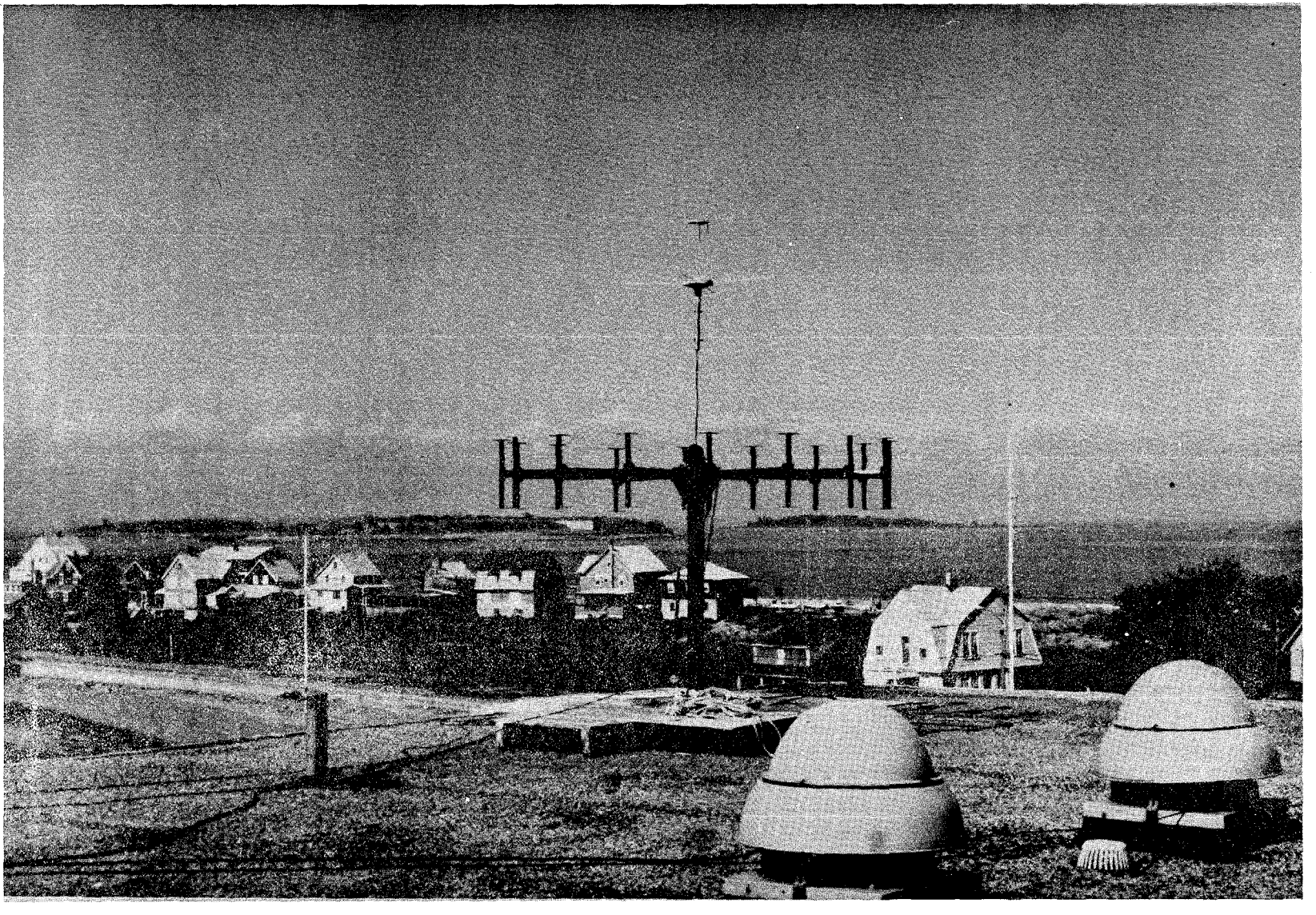

FIGURE 4.13 INSTALLATION OF SERVO CORP. ANTENNA WITH INTECH ANTENNA MOUNTED ABOVE

which was underway but not clear enough to use its homer. Upon reaching open water, the cutter obtained a homer bearing, which was within a few degrees of the initial bearing measured from the station. The cutter proceeded, pausing to search the Southeast shore of intervening Long Island, to home on and recover the first EPIRB. Prior to completion of the first recovery, a second EPIRB was deployed at a point approximately one nautical mile east of Winthrop Highlands (5 nmi from the station) and the cutter was given a bearing to the second EPIRB from Pt. Allerton. This time, since the cutter was not collocated with the land based DF, the cutter's homing bearing was used with the land based bearing to determine the bearing and distance to the EPIRB. Thus, it was not necessary to search the shore of intervening Deer Island on the trip to the second EPIRB. The rescue cutter located and recovered both EPIRBs within one hour after the first alert. Shore bearings taken during the demonstration were within 1°-3° of the actual bearing to the EPIRB.

It should be noted here that, during the set up prior to the demonstration, a graphic demonstration was provided of the capabilities of shore-based direction finding during an actual SAR case. The Coast Guard station was in communication with a vessel that was lost and disoriented. The shore-based direction finding equipment was able to provide a bearing to the vessel, which was used initially by a Coast Guard helicopter to aid in locating the distress, and by the rescue cutter which was also able to home on the vessel's transmissions using the homer that had been installed for the demonstration.

5. CONCLUSIONS AND RECOMMENDATIONS

As stated earlier in Section 2.1, the requirements on which the conclusions below are based are as follows:

a. signal sensitivity - equivalent to VHF receivers presently in use at Coast Guard shore stations;

b. accuracy - $\pm 3°$ degrees rms;

c. mechanical/structural - suitable for installation on unattended antenna towers, over the range of environmental conditions prevalent in the U.S.

Consistent with these requirements, the following conclusions are made:

1. Shore-based DF has been shown to be a valuable potential tool in the accomplishment of SAR mission requirements. Properly implemented shore-based DF can improve reliability and safety of the SAR function by reducing the number of off shore hours necessary to fulfill the mission requirements without increasing station manning requirements.

2. In addition to its usefulness with the present VHF/FM voice transmissions, shore-based DF will enhance the value of VHF/EPIRB system concepts presently under consideration. The reception range from an EPIRB to a homer-equipped surface craft will only be 6-8 miles, due to the relatively low antenna heights available with the smaller cutters. Shore-based DF however, given a suitable antenna location, can provide bearing to EPIRBs 20 miles or more offshore. These bearings can be used to vector surface craft to within reception range of an EPIRB, thus greatly increasing the reliability of EPIRB location, and reducing search time.

3. The evaluation has covered essentially all commercially available units and a number of designs which have been built but are not commercially available. None of these units are suitable to meet Coast Guard requirements without some modification. All units are deficient in one or more of the following areas - range of reception (signal sensitivity); accuracy; and mechanical/structural design.
4. The direction finder performance is critically dependent on its installation and the surrounding environment. Its location must be carefully chosen to provide a clear line of sight over the water. The presence of high buildings, metallic structures or land masses within the signal path can cause serious signal degradation and misleading bearings.
5. An analytical comparison of available direction-finding techniques has determined that the synthetic doppler techniques will provide the best accuracy and least susceptibility to multipath; however, under most conditions an Adcock array will also provide satisfactory performance.
6. In comparing the two available bearing readout techniques, digital and CRT, the latter was found to offer additional information useful in judging the quality of the bearing. The digital readout, on the other hand, will furnish a more accurate bearing on a strong signal. In a typical shore-based installation, the advantages of the CRT display would probably outweigh the small loss in accuracy. However, for a given system, the CRT display will be more costly.
7. The capability of remoting the DF antenna via voice grade telephone line is desirable. Although the majority of installations may not require it, some sites, either because of extreme siting problems at the station or because of the proximity of substantially higher terrain

(e.g, Southwest Harbor/Cadillac Mountain) will find the additional cost of equipment and telephone tolls to be cost effective. Such remoting is a common practice for Coast Guard VHF communications.

As a result of the above conclusions the following recommendations are made:

1. The Coast Guard should proceed with a thorough test and evaluation program, whose output would be the specification for an operational DF, and a plan for its implementation.
2. The installation of the DF will be critical to its correct performance. Since ideally, the reception of an alert via the normal communications system should also be accompanied by a bearing from the site DF, equivalent signal range is highly desirable. Accordingly, the DF antenna height should be the same as the normal communications antenna.
3. The DF antenna location should be carefully chosen for each site, so as to minimize, or at least alleviate, the effects of local signal reflectors. This point cannot be emphasized too strongly. A carefully chosen antenna location is vital to the correct operation of any direction finder, as a poor site can result in severe errors and poor signal reception.
4. The development of a systematic, documented procedure for evaluation of potential sites is recommended. In this way the widely varying site characteristics of the coastal stations can be analytically and/or empirically examined and the optimum choice of site, tower height, and type of DF antenna determined without resort to expensive trial and error techniques.

5. Efforts to improve sensitivity/range of commercially available units would be cost effective and should be undertaken. Incorporation of low noise preamplification and improved filtering will improve sensitivity, thereby easing siting problems and reducing tower height requirements.

To detect signals from proposed EPIRB designs on a par with distress signals from the more powerful VHF-FM voice transceivers, additional gain will be required. Since the EPIRB designs transmit a binary coded signal, processing gain can be achieved by the utilization of correlation detectors in the DF receiver. The use of this technique in enhancing the reception of EPIRB signals has been demonstrated in the receiver developed by TSC for the EPIRB program[1] and should be considered for eventual incorporation in shore-based DF receivers.

6. In the course of the analytical evaluation of direction finding techniques, the IDFM position determination system (described in Appendix B) was brought to our attention. While the system has not been tested experimentally, the analytical results indicate the system may have potential in fulfilling the shore-based DF requirement. It is therefore recommended that an experimental program to evaluate the IDFM concept be considered.

APPENDIX A

EQUIPMENT SPECIFICATIONS

SPECIFICATIONS - Servo Corp of American Model 7010M VHF/FM Marine Direction Finder System

[illegible]	Wide aperture Quasi-Doppler radio direction finder, with electronic commutation.
[illegible]	150 to 174 MHz, with up to 12 crystal-controlled channels.
[illegible]	
Sensitivity	5 μ volts/meter for $\pm 3°$ bearing.
Instrumental Accuracy	$\pm 1°$.
Vertical Angle Coverage	Up to 60°.
Control	Complete digital remote control capability via a single unconditioned bi-directional telephone line pair or telemetry link. Distance unlimited. Audio, if desired, is obtained via a second unconditioned telephone line pair or telemetry channel.
[illegible]	Wide aperture Doppler type, 16 elements. Diameter: 3.14 meters (123.5 in.). Height to center of VHF arm: 1.86 meters (73.2 in.). Overall height: 2.09 meters (82.3 in.). Weight: 67.2 kg (148 lbs.).
[illegible]	
Noise Figure	5-7 dB.
Sensitivity	Better than 10 dB S + N/N for 1.5 microvolt, 30% modulated 400 Hz signal.
Frequency Stability	0.002% min.
Channels	Up to 12 available with either local or remote selection.
Adjacent Channel Separation	50 KHz separation. 6 dB bandwidth, 40 KHz min. 80 dB bandwidth, 70 KHz max.
Rejection	80 dB (image, IF, spurious).
Audio Output	50 mW, 600 ohms.
AGC	Audio output does not vary by more than 3 dB over 80 dB change in input.
Squelch	Automatic signal-activated squelch control.
Processor	Contains circuits for antenna commutation, DF data processing, encode/decode logic and modems for remote telephone line or telemetry link control.
[illegible]	Terminal junction for encode/decode logic and modems for remote control of DF system. Provides interface for display control unit, slave display units and data source for radar interface.
[illegible]	
Bearing Display	3-digit, 7-segment numeric, in one-degree increments.
DF Signal Averaging Time	Operator controlled, ½, 1 and 2 sec.
Controls	12-channel pushbutton selector switch, illuminated for channel verification; QDM/QDR switch and indicator light; storage mode switch; audio volume control; power ON/OFF; dimmer control; lamp test; signal present indicator; system alarm indicator.
[illegible]	
SYSTEM (excluding antenna)	
Ambient Temperature	−10°C to +55°C.
Relative Humidity	Up to 90 ±5%.
Duty	Continuous, unattended.
ANTENNA	
Ambient Temperature	−54°C to +65°C.
Relative Humidity	Up to 100%.
Ice Loading & Wind	12.7 mm (.5 in.) minimum radial ice build-up. 177 KMPH (110 MPH) winds. Antenna safety factor.
Weather	All conditions including fog, rain, sleet and snow.
Duty	Continuous, unattended.
[illegible]	120/220 VAC $^{+10\%}_{-15\%}$, 47-63 Hz.

Source: Servo Corporation of America, Tech Data, Publication 2035

SPECIFICATIONS: INTECH INC. MARINER 360

SPECIFICATIONS

General

Frequency Range	156 to 163 MHz
Channel Capacity	12 crystal controlled
Bearing Accuracy	±2°
Receiver Dimensions	3.7"H X 10"W X 10"D
Weight	6 pounds
Antenna Dimensions	
Height	23"
Width	10" without groundplane dipoles
	48" with groundplane dipoles
Weight	5 pounds
Operation in Relative Winds	Up to 100 Knots
Interconnect Cabling	One run of RG-58A/U and one run of shielded 2-conductor control cable between antenna and receiver-indicator
Controls	Volume ON/OFF
	Squelch
	Channel Selector
	Display Brightness
	Update Rate Adjust
Operating Temperature Range	-20 to +50°C
Input Voltage*	13.6 VDC @ 1 A

Receiver

Sensitivity	0.5 μV for 12 dB SINAD
Stability	Phase locked to incoming signal
Squelch Threshold	0.3 μV
Adjacent Channel Rejection	70 dB min
Intermodulation at Usable Sensitivity	60 dB min
Spurious Response	70 dB min
Modulation Acceptance Bandwidth	±7 kHz min
Audio Frequency Response	6 dB per octave de-emphasis between 300 and 3,000 Hz

Antenna Z = 50 Ω, 3 dB Gain

Mounts on standard 1½" antenna mast.

Source: Intech Incorporated, Data Sheet 761

SPECIFICATIONS

SPECIFICATIONS

SYSTEM PERFORMANCE

System Bandwidth:	148 to 174 MHz.
Modulation Detection:	Narrow-band F.M., A.M., and CW.
Operation:	Fully automatic, including sense-channel for "true direction" determination. Fixed non-rotating type antenna with no moving parts.
Output:	Unambiguous relative compass bearing between antenna axis and location of transmitter, full 360° coverage.
Display:	Narrow-line trace from center to outer edge of circular cathode ray tube, plus audio and field-strength indicators.
Response Time:	Instant display of signal transmissions 150 milli-seconds or longer in duration received from any direction.
Bearing Accuracy*:	± 1° at zero calibration heading, ± 2 to 3° on other headings, under clear line-of-sight conditions.
Signal Detection Range:	Nominally line-of-sight.
Receiver Sensitivity:	Better than 1 microvolt at input terminals for usable direction display.
Selectivity:	± 6.5 KHz at 6db, ± 22.5 KHz at 60db.
I.F. Bandwidth:	13 KHz.
Noise-Bandwidth [Display]:	Less than 100 Hz/channel.

[***Note:** Accuracy stated is for ideal conditions. Adcock antenna arrays such as used with this system are subject to as much as a ± 4° error in addition to spec. above if significant horizontal polarization is present.)

RECEIVER/INDICATOR UNIT

Construction:	Epoxy coated aluminum cabinet with splash-proof sealing; lastest solid-state elements except CRT.
Cabinet Mounting Directions:	See drawing.
Assembly Weight:	Approximately 12 pounds.
Signal Indicators:	3-inch CRT with graduated compass rose; 3-inch speaker; field-strength meter.
Tuning:	
Standard—	10 plug-in crystal channels.
Optional—	a) 10-channel scanner (programmed by std. 10 crystals or 9 crystals plus synthesizer option). b) Frequency synthesizer, 148-174 MHz in 5 KHz increments with ± 2.5 KHz fine tuning (replaces 1 of 10 std. crystal channels).
Controls:	ON/OFF, crystal selection, BFO, and AM/FM detector switches; receiver volume, squelch, and CRT adjustments.
Power Requirements:	
Standard—	12VDC (10-14 VDC range) at 1.2 amperes.
Optional—	a) 110 or 220 VAC/50-60 Hz (in addition to std. 12 VDC). b)24/28 VDC (in lieu of std. 12VDC).
Fittings:	Power input and antenna cable connections on rear panel.
Accessories:	
Included—	12VDC power cable and std. 50 foot long set of 2 antenna cables (JA412CCJF or RG59U coax; specify type).
Optional—	a) Addl. antenna cable length b) Hood for CRT c) Mounting bracket for chassis d) DBR-410 digital bearing readout unit

ANTENNA

Type:	
Standard—	AA-363 Adcock array with 4 dipole elements, integral sense channel, and support mast with guy-lines (for fixed station or shipboard mounting; complete 148-174 MHz bandwidth coverage).
Special Order—	a) FAA-369 Adcock array with 4 monopoles and whiptype sense (for auto roof mounting; ± 1 to 2% bandwidth limitation). b) ADFA-317 crossed loops with integral low-profile sense (for aircraft with retractable landing gear; ± 1 to 2% bandwidth limitation).
Construction:	Metallic with weatherproof sealing and corrosion-resistant coating.
Dimensions:	
Standard AA-363—	See drawing
Special FAA-369—	Flat plate approx. 22 inches square with 17 inches tall by 0.25 inches in diameter monopole and sense elements.
Special ADFA-317—	12.78 inches tall with 6.2 inches in diameter loop array and 8 inches square mounting plate.
Assembly Weight:	
Standard AA-363—	Approximately 15 pounds.
Special FAA-369 and ADFA-317—	Approximatley 5 and 7.5 pounds, respectively.

Source: Ocean Applied Research Corporation, Research Bulletin 1-75

APPENDIX B

IDFM POSITION DETERMINATION SYSTEM (COVERED BY PATENT)*

The techniques considered in the preceding sections are based either on phase comparisons (Doppler and Adcock) or on signal envelope comparisons determined by directional antenna patterns (Homer). A novel technique, invented by Dr. E. J. Baghdady in 1970 and is covered completely by pending patents, will now be briefly described that enables not only high-accuracy determination of direction but also of distance to the source, based entirely on frequency measurements and on "aperture" or "baseline" dimensions on the same order of magnitude as the Rohde and Schwarz system.

The basic principles of this novel technique can be summed up as follows:

Rectilinear, uniform motion of a receiving antenna induces a Doppler shift, in the frequency of an incident signal, proportional to the cosine of the angle of arrival of the incident wave relative to the orientation of the line of motion (LOM) of the receiving antenna. Such rectilinear motion of one receiving antenna can be simulated by commutating the input of the receiver among a number of discrete antenna elements arranged along a straight line of the desired length.

Two colocated, orthogonally oriented LOM's (e.g., one along N-S and one along E-W) give the azimuth angle of arrival, θ, of the incoming wavefront as

$$\tan\theta = \frac{\text{Induced Doppler Shift of E-W LOM}}{\text{Induced Doppler Shift of N-S LOM}}, \qquad (B.1)$$

Two LOM crosses spaced a distance L apart yield the range R to the source as

$$R = Lf_m(D/\lambda)\frac{f_{c2}}{f_{c1}f_{s2} + f_{c2}f_{s1}} \qquad (B.2)$$

*U.S. Patent #4,060,809 and others pending.

where

f_c = Induced Doppler shift of N-S LOM

f_s = Induced Doppler shift of E-W LOM

Subscripts 1 and 2 refer to the two crosses

f_m = number of sweeps of each LOM per second

D = length of each LOM

λ = wavelength of incoming signal carrier.

The RMS errors due to random noise are given by

$$\sigma_\theta \approx \frac{\sigma_f}{f_m D/\lambda} \quad \text{for low elevation angles} \tag{B.3}$$

and

$$\sigma_R \approx 2\frac{R^2}{L} \cdot \frac{\sigma_f}{f_m D/\lambda} \qquad \begin{array}{l}\text{for } R \ggg L \\ \text{and } |\theta| < 60^\circ\end{array} \tag{B.4}$$

where

σ_f = RMS error in frequency count

$$\approx \frac{1}{2\pi} \cdot \frac{1}{T_c} \cdot \frac{1}{\sqrt{S/N}}, \qquad S/N \geq 7 \text{ dB} \tag{B.5}$$

T_c = Frequency counting time interval

S/N = Ratio of average power in signal component whose frequency is being counted, to the average power in the noise contained within the pre-counting noise bandwidth, B_n.

If we consider a situation in which the emitter effective radiated power is one watt average, the receiver noise figure is 6 dB and the product of receiving antenna gain and coupling loss is 0dB, then for

$$f_c = 156.50 \text{ MHz},$$

$$\sigma_R = 2.29 \times 10^{-10} \frac{R^3}{L} \cdot \frac{\sqrt{B_n}}{T_c} \cdot \frac{1}{f_m D/\lambda} \qquad (B.6)$$

Now, if $R = 3 \times 10^4$ m, $L = 10$m, $B_n = 25$ Hz, and $T_c = 1$ sec, then

$$\sigma_R \approx 3 \times 10^3 / (f_m D/\lambda) \text{ m}. \qquad (B.7)$$

The product $f_m D/\lambda$ represents the maximum induced frequency shift caused by unidirectional commutation. Thus, if $f_m D/\lambda = 10^5$ Hz, which can be realized with $D/\lambda = 2$ and $f_m = 50$ kHz, then $\sigma_R \approx 3$ cm. For $f_c = 156.5$ MHz, $D \approx 3.79$ m.

The capability of an IDFM system for resolving multipath or multiple target signals arriving from different directions can be established as follows.

Let the radial angles of arrival of two paths be denoted φ_1 and φ_2 relative to the orientation of the row of commutated antennas. The IDFM imparted to the received signals by the added (simulated) motion of the receiving antenna causes the two to differ in frequency by

$$f_{diff} = f_m (D/\lambda_o)(\cos \varphi_1 - \cos \varphi_2) \text{ (unidirectional commutation)}. \qquad (B.8)$$

If each signal is subject to a pre-counter filtering operation (such as a phase-locked loop) with effective noise bandwidth B_n Hz, the receiver will be capable of separating (resolving) the two signals if

$$|f_{diff}| > B_n \cdot \qquad (B.9)$$

Thus, if we set $\varphi_2 = \varphi_1 = + \Delta\varphi$, where $\Delta\varphi << 1$, then $\cos \varphi_1 - \cos \varphi_2 \approx \Delta\varphi \sin \varphi_1$ and condition (B.9) can be expressed as a condition on $|\Delta\varphi|$, namely

$$|\Delta\varphi| > \frac{1}{|\sin \varphi_1|} \cdot \frac{B_n}{f_m (D/\lambda_o)} \quad \text{(unidirectional commutation)}. \qquad (B.10)$$

This states that if the directions of incidence of replicas of the emitter signal arriving over different propagation paths differ by any amount that exceeds the right-hand member of (B.10), then the receiver will resolve the two signals and count their respective IDFM frequency shifts separately.

As an illustration, if $f_m(D/\lambda_o) = 10^5$ Hz and $B_n = 25$ Hz, the right-hand member of (3.70) is on the order of 2.5×10^{-3} radian.

The above also applies to signals arriving from different emitters that may be radiating at the same or different frequencies. Indeed, by virtue of the directional resolution capability expressed by condition (B.10), an IDFM receiver equipped with an appropriate number of narrow filters (or line-tracking phase-locked-loops) (or one search-and-lock filter) can resolve and determine the positions of a multiplicity of emitters as long as the pairwise differences between the directions of arrival of their signals exceed the quantity expressed by the right-hand member of condition (B.10).

REFERENCES

1. Engels, Peter D., and Charles J. Murphy, VHF-FM Emergency Position Indicating Radio Beacon - Final Report, Report No. CG-D-29-78, Transportation Systems Center, Cambridge MA 02142. In Preparation.

2. Reference Data for Radio Engineers, 5th Edition p. 26-12.

3. Flight Evaluation for Acceptance of the Dorne & Margolin, Inc. DMSE 47-2 UHF/VHF Homing System for the HH-52A Helicopter, U.S. Coast Guard Aircraft Repair & Supply Center, Elizabeth City, N.C. February 1971.